Supremacy of Fully Convolution Neural Network over other Segmentation Algorithms in Prediction of Retinal Diseases

Madhab Paul Choudhury
Research Scholar, PhD(engg.)
IIT ISM Dhanbad
Jharkhand

J Paul Choudhury
Retired Professor(IT), Kalyani Govt Engg. College
Kalyani,, West Bengal
Professor, Narula Institute of Technology, Kolkata

Abstract.
The eye is considered to be the most important sensory organ for humans and it plays a vital role in the overall ability of humans to interact with the world. Unfortunately, many individuals in both rural and urban areas suffer from eye conditions such as cataracts, glaucoma, ocular hypertension, bulgy vision, etc. that affected their vision. There are a variety of causes such as age, diabetes, genetic and inheritance. Modern lifestyles, which have led to increased use of displays for digital devices, are also a factor affecting the vision.
This study aims to develop a predictive model for vision-related diseases by leveraging medical data and analyzing the influence of various contributing factors using deep learning methodologies. Early detection of eye conditions is essential to avoid serious complications, as timely diagnosis plays a critical role in ensuring effective treatment. Conducting thorough assessments to identify potential indicators of eye diseases is highly encouraged. Deep learning and artificial intelligence (AI) significantly enhance the ability to detect these illnesses at an early stage.
The purpose of this research is to lay the foundation for discovering a robust and adaptable solution. Specifically, the study focuses on reviewing the segmentation of eye diseases using advanced deep learning models such as SegNet (Semantic Segmentation), TL-ESM Net(Transfer Learning with Ensemble based Segmentation), FCN(Fully Convolution Network), Deep Lab(Deep Neural Network), U Net, Deep Learn(Deep learning Segment), K-means Clustering, Mask R-CNN(Region based Convolution Neural Network), E Net(Efficient Neural Network), CNN(Convolutional Neural Network) and CRF(Conditional Random Field). The proposed classification framework follows a series of steps: initially, it involves in gathering widely accessible datasets related to eye diseases and performing data preprocessing to ensure consistent experimental conditions. The primary objective is to train the model to accurately identify symptoms of eye diseases, rather than optimizing for a narrow subset of data. Here an effort is being made to work using segmentation algorithms on retinal eye image disease data set with an objective to select a particular model suitable for the analysis of data set. After selecting suitable model, it is necessary to find out the disease affected persons so that in course of time, the concerned person may be recovered with application of proper medicine and food and other items as the case may be.

Keywords.
SegNet(Semantic Segmentation), TL-ESM Net(Transfer Learning with Ensemble based Segmentation) , FCN(Fully Convolution Network), Deep Lab(Deep Neural Network), U Net, Deep Learn(Deep learning Segment), K-means Clustering, Mask R-CNN(Region based Convolution Neural Network), E Net(Efficient Neural Network), CNN(Convolutional Neural Network) and CRF(Conditional Random Field)

1.Introduction.

Image segmentation is a computer vision technique that divides a digital image into multiple segments, or regions, of pixels. These segments represent different objects or parts of objects, making it easier to analyze and process the image. In essence, it's the process of assigning a label to each pixel in an image, grouping similar pixels together based on characteristics like

color, texture, or intensity.

The objective of image segmentation includes simplification of image representation, object detection and recognition, image analysis, pixel grouping and assignment of label to each pixel. Under simplifying Image Representation,Segmentation reduces the complexity of an image by breaking it down into meaningful parts, making it easier to understand and work with.

2. Literature Review.

A multi-scale image-fusion technique markedly enhances dermoscopic analysis by improving the accuracy of classifying benign lesions and detecting melanoma. This method begins by synthesizing two color-normalized versions of the image and applying k-means clustering to each to precisely delineate the lesion boundaries [1]. Spine hemangioma segmentation focuses on the automated identification and localization of tumours within MRI scans[2]. While multiple segmentation techniques are available, this study proposes a U-Net-based method built with PyTorch and fine-tuned using the Adam optimizer.

This study presents a novel ensemble framework for chest disease analysis on X-ray images sourced from the Kaggle repository[3]. It combines three distinct CNN-based classifiers CNN-1, CNN-3, and VGG-16 for disease classification, alongside a U-Net architecture dedicated to lung region segmentation. This research proposes TL-ESMNet, a Transfer Learning-based Ensemble Network designed to tackle the challenges of medical image segmentation[4]. This study integrates fuzzy logic into two conventional threshold-based vessel detection techniques “mean-c thresholding” and “Iso-Data thresholding” resulting in membership masks that assign degrees of vessel-likeness instead of binary labels[5]. Each fuzzy thresholding method is executed separately on fundus images from DRIVE, STARE, and CHASE_DB1 datasets. The proposed method enhances image pixel clustering by integrating Particle Swarm Optimization (PSO) with the K-Means algorithm. Among the combined approaches, K-Means paired with PSO delivers superior results, outperforming the combination of K-Means with the Firefly Algorithm[6].

This study presents CoTr, a novel hybrid framework that blends convolutional neural networks (CNNs) with transformers to enhance 3D medical image segmentation accuracy[7]. The CNN component first extracts rich feature representations, while an efficient *deformable transformer* (DeTrans) models long-range dependencies across multi-scale feature maps. The proposed method introduces a distinctive potential function that integrates data from both superpixel segmentation and edge detection[8]. By combining these two sources, the model can capture features across multiple scales while minimizing the impact of inaccuracies that may arise from superpixel segmentation alone. This study offers a comprehensive overview of Otsu’s thresholding method, a cornerstone in computer vision and image processing used to segment images by distinguishing meaningful structures[9].

To enhance the detection of spondylolisthesis in X-ray images, this study leverages deep learning methodologies[10]. Specifically, the YOLO (You Only Look Once) framework is employed due to its real-time processing capabilities and high accuracy.

To process the datasets, various preprocessing methods—including discretization, resampling, principal component analysis (PCA), and decision tree-based techniques have been employed. For classification, several machine learning algorithms have been utilized, including Support Vector Machines (SVM), K-Nearest Neighbors (KNN), Naïve Bayes (NB), Decision Tree (DT), and Random Forest (RF), all implemented using 10-fold cross-validation[11]. The objective of this research is to enhance the accuracy of heart disease prediction while minimizing the number of input attributes[12]. An effective early detection system is crucial for mitigating the risks and complications associated with diabetes, thereby promoting healthier lifestyles[13]. This study introduces an ensemble learning approach for early diabetes prediction, utilizing the AdaBoost algorithm with Support Vector Classifier (SVC) and Decision Tree (DT) as base estimators. A recent study presents a convolutional neural network

(CNN)-based model designed to predict melanoma skin cancer from patient skin lesion images[14]. This paper[15] introduces a method for detecting cardiovascular disease using the XGBoost algorithm in combination with OPTUNA for hyperparameter optimization.

This study introduces an innovative deep convolutional neural network (DCNN) framework for classifying skin cancer lesions[16]. The model is tested on two imbalanced datasets—HAM10000 and ISIC-2019—and its performance is benchmarked against several popular transfer learning models, including VGG16, VGG19, DenseNet121, DenseNet201, and MobileNetV2. To tackle the challenge of imbalanced training data, this study incorporates an improved focal loss function into the proposed model architecture[17]. A recent study introduces an advanced deep learning framework that significantly enhances the diagnosis of COVID-19, Lung Opacity, and Viral Pneumonia using chest X-ray (CXR) images[18].

This study introduces a data-flow framework designed to support two types of research while adhering to data protection standards set by the ethics committee overseeing human subject studies[19]. This study introduces EffiFusion-Net, a multimodal deep learning framework designed to classify stress severity by integrating facial and physiological data[20]. A recent study presents the Residual Attention Neural Network for Breast Cancer Classification (RANN-BCC), a deep learning model designed to assist medical professionals in diagnosing breast cancer, specifically differentiating between Invasive Ductal Carcinoma (IDC) and non-IDC cases using whole slide imaging (WSI)[21].

An automated system using deep learning techniques has been developed to detect diseases in guava leaves[22]. The study has been conducted on a dataset of 4,046 images, classified into seven distinct disease categories. The performance of traditional machine learning methods against deep learning approaches has been evaluated, including vision transformers and transfer learning. The findings clearly show that deep learning significantly outperforms traditional techniques. While the SVM model has achieved around 78% accuracy, deep learning models surpassed 90%. Transfer learning has reached approximately 97% accuracy, and the vision transformer has achieved the highest accuracy at 98%. These results highlight the potential of deep learning for early and accurate disease detection in guava cultivation.

To bridge the existing gap in breast cancer diagnostics, the proposed research leverages machine learning to automate detection processes, specifically tailoring models to the unique characteristics of Indian breast tissue and incorporating metadata to enhance assessment accuracy [23]. The methodology of this study[24] involves an extensive evaluation of multiple algorithms, from which three—Support Vector Machine (SVM), Logistic Regression, and K-Nearest Neighbours (KNN) have been selected based on their superior performance.

To tackle the challenge of multi-class lung disease detection, an innovative model has been introduced that integrates a Depth-wise Separable Convolutional Neural Network (DSCNN) with a Multilayer Perceptron (MLP) to classify COVID-19, non-COVID pneumonia, and lung cancer using CT images[25].

This study introduces a two-stage deep learning framework for pancreatic cancer detection using CT imaging[26]. This study presents a systematic comparative analysis of various supervised machine learning (ML) algorithms for heart disease prediction and introduces a blueprint for a Dietary Approaches to Stop Hypertension (DASH) lifestyle change therapy recommendation system[27].

In this study, the authors [28] have explored six machine learning algorithms alongside three feature extraction techniques—Image Loading, Histogram of Oriented Gradients (HOG), and Local Binary Patterns (LBP)to determine the most effective combination for brain tumor detection and classification. Experiments have been conducted using two publicly available Brain Tumor MRI datasets from Kaggle. This study presents a comprehensive evaluation of seventeen machine learning models aimed at optimizing predictive performance for classification tasks[29]. A key focus is on addressing challenges related to feature selection

and class imbalance.

This review[30] explores the pre processing techniques employed, the advanced models applied, and their corresponding performance in Parkinson's disease (PD) diagnosis. The evaluation covered a range of algorithms, including Support Vector Machines (SVM), Random Forests (RF), and Convolutional Neural Networks (CNN).

This study[31] presents a comprehensive approach to classifying arrhythmias using electrocardiogram (ECG) signals, focusing on five categories: Normal (N), Fusion (F), Supraventricular (S), Ventricular (V), and Unknown (Q).

This study[32] offers a comprehensive evaluation of Explainable Artificial Intelligence (XAI) methods, organized by data types—namely imaging, genomic, and clinical. It includes a detailed comparison of prominent XAI techniques such as LIME (Local Interpretable Model-agnostic Explanations), SHAP (SHapley Additive exPlanations), and Grad-CAM. Additionally, it outlines key challenges and proposes future research directions.

This study[33] introduces a 14-layer Bidirectional Long Short-Term Memory (BiLSTM) neural network designed for automatic image captioning.

This study[34] proposes an innovative hybrid model that combines DenseNet201-based transfer learning with a Bayesian-Optimized Fast Learning Network (FLN) for classifying breast cancer from ultrasound images.

This study provides a comprehensive systematic literature review (SLR) on the application of deep learning (DL) techniques for lung cancer diagnosis and classification, utilizing various medical imaging modalities such as X-rays, whole slide imaging (WSI), computed tomography (CT) scans, and magnetic resonance imaging (MRI)[35].The review focuses on publications from 2015 to 2024, offering insights into methodologies, advancements, quality assessments, and tailored DL approaches in the field.

This study offers an in-depth analysis of recent advancements in machine learning and deep learning techniques for diabetes detection and classification[36].

Recent DL approaches for lung cancer diagnosis have primarily leveraged convolutional neural networks (CNNs) due to their capacity for automatic feature learning and hierarchical representation of image data[37].

Between 2018 and 2023, significant advancements have been made in applying deep learning (DL) techniques for lung cancer detection, particularly using convolutional neural networks (CNNs)[38]. This period has seen the development of various models, the utilization of diverse datasets, and the integration of explainable AI (XAI) methods to enhance the interpretability and reliability of diagnostic tools. Our proposed model harnesses the advantages of multiple pre-trained networks by freezing the initial convolutional layers and fine-tuning the deeper ones, allowing for effective feature extraction and increased robustness. This research presents a deep learning-based approach for classifying squamous epithelial cells into five distinct categories, thereby facilitating a detailed assessment of cervical cancer severity[40].

A novel approach has been introduced to enhance the detection of thyroid cancer using ultrasound imaging[41].This method employs a Channel Boosted Convolutional Neural Network (CB-CNN) to improve diagnostic accuracy and reduce error rates.

The authors obtained high classification accuracies across various datasets, demonstrating the effectiveness of their proposed approach[42].

A novel multi-stage architecture has been introduced to enhance cervical cancer screening through advanced image classification techniques[43].This approach begins by utilizing three pre-trained models to analyze medical images. In this study, the authors use the Herlev dataset, which comprises cervical cell images along with associated disease symptoms, to enhance the classification and diagnosis of cervical cancer[44]. The dataset undergoes preprocessing steps, including imputation to address missing values. Image preparation involves standard techniques such as cropping, resizing, flipping, and rotation to ensure consistency and quality.

This study introduces a comprehensive approach to enhancing cervical cancer diagnosis by leveraging cutting-edge deep learning techniques[45].Specifically, it evaluates the performance of 40 convolutional neural network (CNN) models and over 20 vision transformer (ViT) models on the SIPaKMeD Pap smear dataset, marking it as one of the most extensive comparative analyses in this domain. This study employs a comprehensive Pap smear image dataset to develop an efficient cervical cancer diagnostic system[46]. Feature extraction has been performed using several pre-trained convolutional neural network (CNN) models, including ResNet101, ResNet50, DenseNet121, DenseNet169, DenseNet201, VGG16, VGG19, and MobileNet, as well as their hybrid combinations. To reduce computational load while retaining essential information, Principal Component Analysis (PCA) has been applied to retain 95% of the data variance. This study introduces an advanced diagnostic framework for detecting invasive ductal carcinoma (IDC) in breast tissue using whole slide images (WSIs)[47].The methodology has been evaluated on a dataset comprising specimens from 162 patients diagnosed with IDC. The framework leverages various convolutional neural network (CNN) architectures, including EfficientNet, EfficientNetV2, and VGG16, to analyze the histopathological images.

This study[48] introduces an advanced diagnostic framework for lung cancer classification, termed "Optimal DenseNet," which integrates DenseNet architecture with the Modified Golf Optimization (MGO) algorithm.The MGO algorithm fine-tunes hyper parameters such as the number of hidden units, layers, and convolutional filter sizes to enhance model performance.

The manuscript [49] introduces a CNN-based normalized architecture integrated with Bayesian Optimization and Long Short-Term Memory (CNN-BO-LSTM) for liver cancer detection. In this study, a novel two-stage model named FireNet-MLstm is proposed for efficient and accurate medical image classification[50]. The first component, **FireNet**, incorporates fire modules to significantly reduce the model's size and parameter count, enabling faster classification.

This study introduces an enhanced deep learning framework for improving liver tumor diagnosis using CT images [51]. Initially, both benchmark and manually collected datasets undergo preprocessing through histogram equalization and median filtering to enhance image quality. The proposed model by authors[52] is composed of several key components: a feature extraction module that captures multi-level representations of liver lesions, a **feature** fusion attention module that integrates contextual information across different MRI sequences, and an attention-guided data augmentation module that enhances the training data quality and diversity.

To improve interpretability, the model incorporates Gradient-weighted Class Activation Mapping (Grad-CAM), an explainable AI technique that highlights regions in CT images influencing the model's predictions[53].This visualization aids clinicians in understanding and validating the model's decisions, thereby supporting more informed treatment planning .

A Comparative study of the performance of Machine Learning models with cross validation techniques has been made for the prediction lever disease [57].

Summary of Literature Review are as Follows:-

Table 1

Data Set used Contributions by authors and Remarks in Literature Review

References	**Year**	**Data Set**	**Contributions**	**Remarks**
[1]	2025	Dermoscopic Skin Image	By combining two color-corrected versions, creating conclusive skin lesion	A very detailed picture of the skin lesion is produced by combining the resultant

			delineation by k-means clustering, and leveraging inherent texturalinformation acquired through the Gabor filter.	three-segmented images, demonstrating the complexity of this cutting-edge dermoscopic image processing technique.
[2]	2025	MRI dataset	This introduces a U-Net-based approach, implemented in PyTorch and optimized with the Adam optimizer.	The model has been trained on a substantial dataset spanning the three primary anatomical planes used in medical imaging—Axial, Coronal, and Sagittal without additional data augmentation.
[3]	2025	Chest X Ray Image	Thispaper reports a new ensemble approach that utilizes CNN-1, CNN-3 and VGG-16 structures to classify the disease and U-Net for segmenting the chest diseases in X-ray pictures considered from the Kaggle repository.	The proposed model has been evaluated onperformance metrics like F1-score, Precision, and Recall. Therefore, this result may lead the way for enhanced diagnostic accuracy and treatment decisions in clinical settings
[4]	2025	Breast Tumor Image Dataset	This study introduces a Transfer Learning based Ensemble Net (TL-ESMNet), a novel framework that incorporates adaptive segmentation with attention mechanisms within the Ensemble Net (ESM-Net)stage to address these complexities.	Segmentation has been performed using U-Net or DeepLabV3, leveraging multi-scale feature extraction to ensure accurate tumor boundary delineation.
[5]	2025	Fundus Image of Eye	It has been incorporated fuzzy concepts into two threshold-based vessel detection methods, namely “mean-c thresholding” and “Iso-Data thresholding,”.	The fusion is performed using fuzzy union operation. Experiments are carried out with Fundus images from DRIVE, STARE and CHASE_DB1 databases.
[6]	2023	Plant leaf Image data set	The suggested approach clustersimage pixels by combining Particle Swarm Optimization with K-Means.	The firefly algorithm needs to be altered or combined with other algorithms in order to be used to a wide range of problems.
[7]	2023	3D Medical Image	a novel framework has been presented for accurately segmenting 3D medical images based on the combination of a convolutional neural network and a transformer	As a self-attention device, the transformer performs a global operation where it draws information from all the information on the system in order to make a decision

			(CoTr). .	
[8]	2024	Satellite Image	The proposed approach utilizes a unique potential function that merges information from both super pixel segmentation and edge detection.	The inclusion of edge details extracted via the Sketch token algorithm refines object boundaries, yielding more accurate segmentation results.
[9]	2025	Medical images of patients with paralysis	This proposed work provides a thorough examination of Otsu's approach, covering its algorithmic implementation, mathematical underpinnings, and empirical testing on a variety of image datasets.	The method's shortcomings have been investigated in more detail and suggested improvements, including multi-level thresholding and preprocessing stages to deal withreal-world issues like noise and uneven lighting.
[10]	2025	X Ray Images	To improve the detection of spondylolisthesis in X-ray images using deep learning techniques have been used. YOLO (you only look once) has been used.	The results obtained by YOLOV8 have been compared with that of YOLOV11.
[11]	2019	datasets, viz. Chronic Kidney Disease (CKD), Cardiovascular Disease (CVD), Diabetes, Hepatitis, Cancer, and Indian Liver Patient Disease (ILPD	Several machine learning algorithms have been utilized, including Support Vector Machines (SVM), K-Nearest Neighbors (KNN), Naïve Bayes (NB), Decision Tree (DT), and Random Forest (RF), all implemented using 10-fold cross-validation	The experimental findings indicate that the proposed predictive model achieves improved performance across various metrics, delivering higher accuracy as compared to existing approaches.
[12]	2023	Heart Disease Data Set	An ensemble approach that combines Random Forest with a genetic algorithm for optimal feature selection.	Among the evaluated models, the combination of Support Vector Machine (SVM) and K-Nearest Neighbors (KNN) has delivered the highest performance, achieving an accuracy of 99.36%,
[13]	2022	Diebetes Data Set	This study introduces an ensemble learning approach for early diabetes prediction, utilizing the AdaBoost algorithm with Support Vector Classifier (SVC) and Decision Tree (DT) as base estimators	The model's performance is evaluated using various classification metrics, demonstrating its efficacy in early diabetes detection.

[14]	2025	Skin Cancer Image Dataset	A convolutional neural network (CNN)-based model is designed to predict melanoma skin cancer from patient skin lesion images	The proposed model has demonstrated strong performance, achieving an accuracy of approximately 92%, surpassing existing methods.
[15]	2025	UCI Cleveland dataset, Kaggle Heart Failure dataset	For detecting cardiovascular disease, the XGBoost algorithm in combination with OPTUNA for hyperparameter optimization is used	The proposed approach has achieved an accuracy of 96.77% on the UCI Cleveland dataset and 93.52% on the Kaggle Heart Failure.
[16]	2024	HAM10000 and ISIC-2019	An innovative deep convolutional neural network (DCNN) framework is proposed.	The results reveal that the proposed DCNN model surpasses the compared deep learning models, achieving top accuracies of 98.5% on HAM10000 and 97.1% on ISIC-2019.
[17]	2024	Chest X Ray images	A unique attention mechanism is integrated with ResNet to highlight salient features crucial for pneumonia detection.	The study also provides valuable insights for future work in medical image analysis and machine learning applications in healthcare.
[18]	2025	Chest X Ray images	This model synergistically combines the Vision Transformer (ViT) for capturing long-range dependencies, DenseNet201 for robust feature extraction, and Global Average Pooling (GAP) to preserve essential spatial information.	In COVID-19 it has achieved an accuracy of 99.4% and an F1-score of 98.43%. In Lung Opacity, it has recorded an accuracy of 96.45% with an F1-score of 93.64%. In Viral Pneumonia, it has attained an accuracy of 99.63% and an F1-score of 97.05%. In Normal Cases it has secured an accuracy of 95.97% alongside an F1-score of 95.87%.
[19]	2021	Stress signals are either collected in ambulatory settings, which can be limited to the period of presence in the hospital, or in	The research focuses on the detection and binary classification of stress events using three different machine learning models.	Among the tested models, the best-performing configuration achieves an F1 score of 0.71, significantly outperforming the random baseline of 0.48.

		continuous mode in the field.		
[20]	2025	Stress-related facial features, Physiological signals, such as heart rate and blood pressure.	The model employs an EfficientNet-based convolutional neural network (CNN) for extracting stress-related facial features, enhanced through multi-scale feature fusion.	a weighted soft-voting ensemble classifier is utilized, combining multi-layer perceptron (MLP), k-nearest neighbors (KNN), and random forest (RF) algorithms for better performance.
[21]	2023	Breast Cancer Data Set	The Residual Attention Neural Network for Breast Cancer Classification (RANN-BCC), a deep learning model is designed in diagnosing breast cancer, specifically	RANN-BCC has achieved an accuracy of 92.45%, recall of 0.98, precision of 0.91, and an F1-score of 0.94. These results surpass those of other models tested, such as CNN, AlexNet, ResNet34, and Feed-Forward Neural Networks.
[22]	2025	4046 Guava leaf images	The SVM model has achieved around 78% accuracy, deep learning models surpassed 90%. Transfer learning has reached approximately 97% accuracy, and the vision transformer has achieved the highest accuracy at 98%.	These results highlight the potential of deep learning for early and accurate disease detection in guava cultivation
[23]	2025	INbreast dataset	machine learning models are used to automate breast cancer detection	The most effective single model has achieved a per-image Area Under the Curve (AUC) of 0.95, while an ensemble of four models has increased the AUC to 0.98, with a sensitivity of 86.7% and specificity of 96.1% on an independent test set from the INbreast database
[24]	2025	Breast Cancer Dataset	Support Vector Machine (SVM), Logistic Regression, and K-Nearest Neighbors (KNN) have been used and selected based on their superior performance.	To optimize performance, the Principal Component Analysis (PCA) and Neighborhood Component Analysis (NCA) have been used.
[25]	2025	CT Images	To tackle the challenge of multi-class lung disease detection, an innovative model has been introduced that integrates a Depth-wise Separable Convolutional	The proposed model has been tested on publicly available CT image datasets, encompassing four classes: normal, COVID-19, pneumonia, and lung cancer.

			Neural Network (DSCNN) with a Multilayer Perceptron (MLP) to classify COVID-19, non-COVID pneumonia, and lung cancer using CT images	The system has been implemented in Python 3, and performance has been evaluated using standard metrics, including accuracy, sensitivity, specificity, precision, recall, and F1 score.
[26]	2024	CT Images	This study introduces a two-stage deep learning framework for pancreatic cancer detection using CT imaging. In the second stage, the cropped regions undergo segmentation using various models, viz. UNet, VNet, SegResNet, and HighResNet, to accurately delineate cancerous areas	The models have been trained and evaluated on a private dataset provided by the Champalim aud Foundation in Portugal. Performance assessments, both quantitative and qualitative, indicate that YOLOv5 excels in pancreas localization, while the 2.5D HighResNet model outperforms others in segmentation tasks.
[27]	2024	Heart Disease Data Set	This work presents a systematic comparative analysis of various supervised machine learning (ML) algorithms for heart disease prediction	The performance of these algorithms has been compared, focusing on accuracy as the primary evaluation.
[28]	2024	Brain Tumor MRI datasets from Kaggle	Feature extraction techniques viz. Image Loading, Histogram of Oriented Gradients (HOG), and Local Binary Patterns (LBP) have been used.	Random Forest algorithm has delivered the highest classification accuracy of 99%. Support Vector Machine (SVM) and Logistic Regression has demonstrated good performance.
[29]	2025	Thyroid disease data set	To mitigate class imbalance, random oversampling has been employed, which significantly enhanced classification outcomes. The ensemble model is utilizing a hard voting strategy with integrated multiple classifiers to improve prediction stability and accuracy.	The XGBoost algorithm, combined with SelectKBest for feature selection, has achieved outstanding results
[30]	2025	Parkinson's disease data set	The evaluation has covered a range of algorithms,	Medical imaging supported by deep learning (DL)

			including Support Vector Machines (SVM), Random Forests (RF), and Convolutional Neural Networks (CNN).	methods has significantly enhanced Parkinson's disease detection capabilities
[31]	2025	ECG Arrhythmia Classification Dataset	The methodology integrates advanced signal processing, feature extraction, and deep learning techniques to enhance classification accuracy.	The ACO-optimized Bi-LSTM (ACoBi-LSTM) and FCN (ACoFCN) models have achieved impressive classification accuracy.
[32]	2025	Breast Cancer Data set	It includes a detailed comparison of prominent XAI techniques such as LIME (Local Interpretable Model-agnostic Explanations), SHAP (SHapley Additive exPlanations), and Grad-CAM	Additionally, it outlines key challenges and proposes future research directions
[33]	2025	Flickr and MSCOCO dataset	The model is trained on the ImageNet dataset, utilizing the MobileNet architecture to optimize performance and manage computational demands.	BiLSTM model has been chosen against five other LSTM-based models. Performance evaluation metrics including Precision, Accuracy, Recall, F-score, and Loss Function have been used.
[34]	2025	Breast ultrasound images	DenseNet201-based transfer learning with a Bayesian-Optimized Fast Learning Network (FLN) has been nused for classifying breast cancer from ultrasound images	The model has achieved notable performance metrics: an accuracy of 96.79%, F1 score of 94.71%, precision of 96.81%, and recall of 93.48
[35]	2024	Breast Ultrasound images	The application of deep learning (DL) techniques for lung cancer diagnosis and classification, utilizing various medical imaging modalities such as X-rays, whole slide imaging (WSI), computed tomography (CT) scans, and magnetic resonance imaging (MRI) have been presented.	Under performance Metrics such as precision, accuracy, specificity, sensitivity, and Area Under the Curve (AUC) have been used to evaluate model performance
[36]	2024	Pima Indians Diabetes Dataset	Machine learning and deep learning techniques have been used for diabetes detection and classification	Performance Metrics such as precision, accuracy, specificity, sensitivity, and Area under the Curve (AUC)

				have been used to evaluate model performance
[37]	2025	Chest X-rays (CXR), CT scans, and whole-slide images (WSI)	This paper focusses on analyzing the latest work related to lung cancer detection using deep learning.	convolutional neural networks (CNNs) has also been used here.
[38]	2024	LIDC-IDRI, NLST, the Cancer Genome Atlas (TCGA).dataset	Between 2018 and 2023, significant advancements have been made in applying deep learning (DL) techniques for lung cancer detection, particularly using convolutional neural networks (CNNs).	During this period the development of various models, the utilization of diverse datasets, and the integration of explainable AI (XAI) methods have been used to enhance the interpretability and reliability of diagnostic tools.
[39]	2025	4096 images from SimpakMed, available on Kaggle,	Combination of Convolutional Neural Network (CNN), AlexNet, and SqueezeNet architectures have been implemented. Individually, these models have achieved classification accuracies of 90.8%, 92%, and 91%, respectively.	The ensemble technique of Convolutional Neural Network (CNN), AlexNet, and SqueezeNet has outperformed the individual models, attaining an accuracy of 94%.
[40]	2025	Dementia dataset	A range of traditional machine learning algorithms has been applied to demographic data, with Gaussian Naïve Bayes achieving the highest accuracy of 91.30%.	The SHapley Additive exPlanations (SHAP) framework has been employed to interpret the models, revealing that Normalized Whole Brain Volume (nWBV) has played a notably variable role in influencing predictions across different models.
[41]	2025	Thyroid cancer dataset	Channel boosted-Convolutional Neural Network (CB-CNN) is developed to identify thyroid cancer.	The images undergo segmentation using SegNet, a deep learning architecture is designed to identify and delineate the tumor regions within the thyroid gland.
[42]	2025	Oxford Parkinson's Disease Detection Dataset, Alzheimer Parkinson Diseases 3-	The ensemble methods with feature selection has been used on four data sets. For the Oxford Parkinson's Disease Detection Dataset, the model has achieved an accuracy of 95.67%, with 97.59% precision, 84.5%	In the Circle category, the stacking ensemble has demonstrated exceptional effectiveness by achieving 100% in all evaluated performance metrics. In the Meandercategory, theBase-P16-224 model has attained

		Dataset, New HandPD dataset, Voice Recordings (MDVR-KCL)dataset	recall, 99.32% specificity, and an F1-score of 90.57%. In the Alzheimer Parkinson Diseases 3-Class Dataset, accuracy of 99.85%, precision and recall of 99.81%, specificity of 99.86%, and an F1-score of 99.81%.	97.35% accuracy, 99.26% precision, 95.71% recall, 99.19% specificity, and an F1-score of 97.45%. For the Spontaneous Dialoguedataset, the model has achieved 94.03% accuracy, 92.83% balanced accuracy (BAC), 90.78% precision, 100.0% recall, and an F1-score of 85.67%.
[43]	2025	SIPaKMeD dataset,	This approach begins by utilizing three pre-trained models to analyze medical images.Subsequently, an advanced fusion technique combines the predictions from these models, taking into account the confidence scores of each base classifier to inform the final decision-making process. fusion strategies	To improve the performance of the models, the framework incorporates sophisticated data augmentation methods, including CutMix, CutOut, and MixUp.These techniques enhance the diversity and robustness of the training data, leading to improved model generalization.
[44]	2025	Herlev dataset	For feature extraction, a Stacked Bi-LSTM network is employed to eliminate irrelevant and redundant information, Classification is carried out using a Spiking Neural Network (SNN) optimized with the Deer Hunting Optimization Algorithm (DHOA),	The proposed method is evaluated using multiple performance metrics, achieving an accuracy of 98.21%, sensitivity of 98.27%, specificity of 98.15%, and an F1-score of 98.54%, indicating the robustness and reliability of the approach
[45]	2023	SIPaKMeD Pap smear dataset	It evaluates the performance of 40 convolutional neural network (CNN) models and over 20 vision transformer (ViT) models on the SIPaKMeD Pap smear dataset.	The experimental results reveal that the latest ViT-based models outperform traditional CNN models in terms of classification accuracy..
[46]	2025	Cervical cancer data	Feature extraction has been performed using several pre-trained convolutional neural network (CNN) models, including ResNet101, ResNet50, DenseNet121, DenseNet169, DenseNet201, VGG16, VGG19, and MobileNet, as	High-pass filtering has been also used to enhance feature quality. The proposed model, which integrates ResNet101, DenseNet121, and DenseNet169 features with a soft voting ensemble classifier, has achieved a classification accuracy of **97.03%** for binary

			well as their hybrid combinations.	classification and **96.67%** for five-class cervical cancer classification
[47]	2025	Breast tissue using whole slide images (WSIs)	The framework leverages various convolutional neural network (CNN) architectures, including EfficientNetV2, EfficientNet and VGG16, to analyze the images.	These findings highlight the potential of integrating advanced CNN architectures into diagnostic workflows for breast cancer,
[48]	2024	Lung Cancer Images	An advanced diagnostic framework for lung cancer classification, termed "Optimal DenseNet," which integrates DenseNet architecture with the Modified Golf Optimization (MGO) algorithm.	Comparative analyses indicate that the Optimal DenseNet model outperforms traditional methods, demonstrating its efficacy in accurate lung cancer classification.
[49]	2024	magnetic resonance imaging (MRI) scan images	A CNN-based normalized architecture integrated with Bayesian Optimization and Long Short-Term Memory (CNN-BO-LSTM) has been introduced for liver cancer detection.	The proposed framework, which combines CNN-based ROI feature extraction with LSTM classification and is fine-tuned through Bayesian optimization, demonstrates superior performance as compared to traditional existing methods.
[50]	2022	CT Images	A novel two-stage model named FireNet-MLstm is proposed for efficient and accurate medical image classification.	A new loss function, referred to as G-loss, is introduced to enhance training efficiency.
[51]	2023	CT Images data	Liver segmentation is performed using adaptive thresholding combined with level set methods.	The selected features are then input into a Hyperparameter-tuned Improved Deep Neural Network (HI-DNN), which is also optimized using the GW-CTO algorithm.
[52]	2024	Focal Lever dataset	Several key components: a feature extraction module that captures multi-level representations of liver lesions, a feature fusion attention module that integrates contextual information across different MRI sequences, and an attention-guided data augmentation module that	The framework offers a reliable and effective tool to assist radiologists in accurately classifying liver lesions in real-world clinical applications.

			enhances the training data quality and diversity.	
[53]	2024	IQ-OTH/NCCD dataset	A recent study has introduced the MobileNetV2-SGRU model, which combines the lightweight MobileNetV2 architecture with a stacked Gated Recurrent Unit (SGRU) to enhance lung cancer classification.	The integration of MobileNetV2-SGRU with Grad-CAM offers a robust and interpretable tool for lung cancer diagnosis, combining high accuracy with enhanced transparency.

3. Motivation.

The research work related to image segmentation has been carried out in ([1] - [10]). Out of these Segmentation related to skin in [1], detection of tumor boundary in [2], related to chest pathology in [3], in breast tumor in [4], segmentation of blood vessel in [5], segmentation of plant leaf in [6], segmentation of medical image in [7], segmentation of aerial image in [8], segmentation of images of paralysis affected patients in [9], related to diagnosis of spondylosis from lumbar spine in [10]. The research work of Heart Disease Prediction in ([12], [27]), that of Breast Cancer Disease in ([10], [21], [23],[24],[34])Diabetics Detection([[13], [36]).Skin Cancer Disease Detection in ([14],[16]), Stress Detection([19],[20]), Parkinson Disease Detection([30],[42]), Lung cancer disease Detection ([35], [37], [38], 48], [49],[53]), Cervical Cancer Detection([39], [43], [44], [45], [46]), Lever Tumor detection([51]).

Deep Learning models have been applied in ([20], [21], [36], [35], [38],[45], [48], [49], [53]).Data Mining models in ([4]), Ensemble Learning models in ([9], [11], [24], [38]). Machine Learning Models in ([12], [13], [22], [23], [28], [29], [36], [46]). Segmentation algorithms in ([26], [41]).

However, no author has worked on the same data set and not evaluated using several evaluation measures. That is the reason for this proposed work which has been written in this paper. Here an effort is being made to work using segmentation algorithms on retinal eye image disease data set with an objective to select a particular model suitable for the analysis of data set. After selecting suitable model, it is necessary to find out the disease affected persons so that in course of time, the concerned person may be recovered with application of proper medicine and food and other items as the case may be.

4. Data set.

The retinal fundus image data set has been collected from Kaggle Repository ([56]). A retinal fundus image, also known as a fundus photograph, is a picture of the back of the eye, specifically the inner surface, which includes the retina, macula, optic disc, and blood vessels. It helps eye care professionals diagnose and monitor various eye conditions and diseases. The term "fundus" refers to the back, inner surface of the eye, where the retina is located.

The image data set comprises of training, testing and validation data sets. Each image data set comprises of 5 types. The images of five classes of diseases are furnished in figure 1. The description of each class is furnished in figure 2. These are furnished below:-

Table 2

Retina Fundus Image Data Set

No	Image type	Image related Information
1	Bulging eyes	Bulging eyes, medically known as exophthalmos or proptosis. This refers

		to an abnormal forward displacement of one or both eyeballs.
2	Cataract	A cataract forms when proteins in the eye's lens aggregate, leading to cloudiness. This clouding disrupts the passage of light into the eye, causing blurred vision and other visual impairments.
3	Crossed-eyes	Strabismus—commonly called crossed eyesis a condition where the eyes aren't aligned properly and don't focus on the same target simultaneously. One eye may drift inward, outward, upward, or downward due to poor coordination among the eye muscles, nerve signals, or brain control.
4	Glaucoma	Glaucoma is identified using several eye tests that evaluate the optic nerve and nearby areas. Key to diagnosis are images of the fundusthe back part of the eyeparticularly the optic disc and cup.
5	Uveitus	Uveitis refers to inflammation of the uvea, the eye's middle layer made up of the iris, ciliary body, and choroid. It often leads to symptoms like redness, pain, and blurred vision.

Images of Bulging eyes

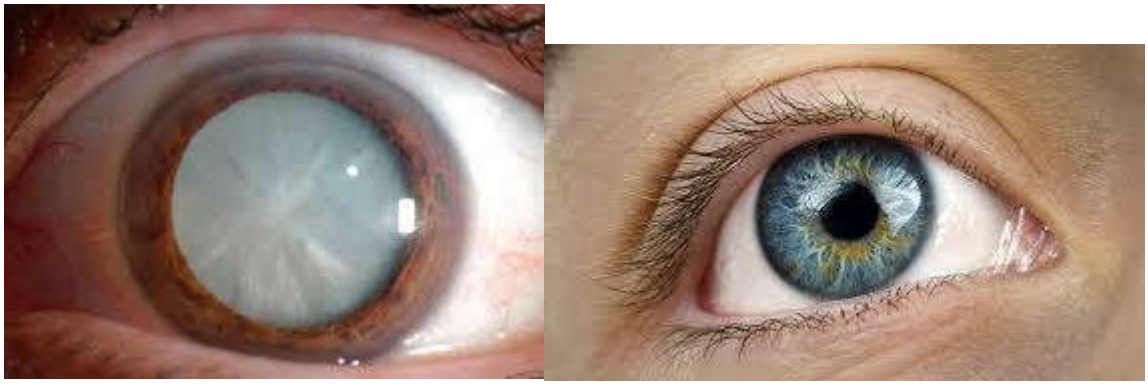

Images of Eye Cataracts

Images of Crossed Eyes

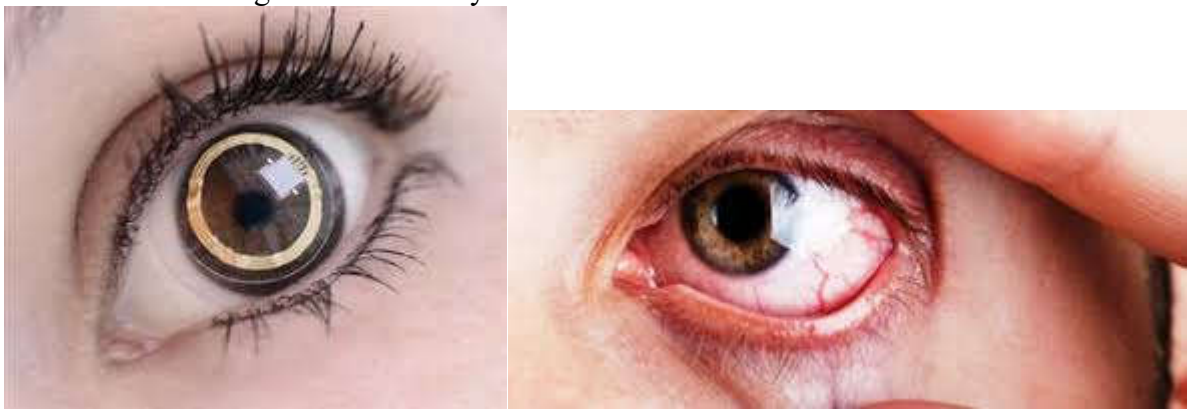

images of eye Glaucoma

Images of Uveitus

Figure 1: Images of Retinal Diseases

5. Methodology.

5.1. SegNet.

SegNet is a deep convolutional neural network architecture designed for semantic segmentation, which involves in classifying each pixel in an image into a predefined category. It is characterized by its encoder-decoder structure, mirroring the first 13 layers of the VGG16 network in the encoder. SegNet is particularly useful in applications like autonomous driving, medical image analysis, and urban scene understanding.

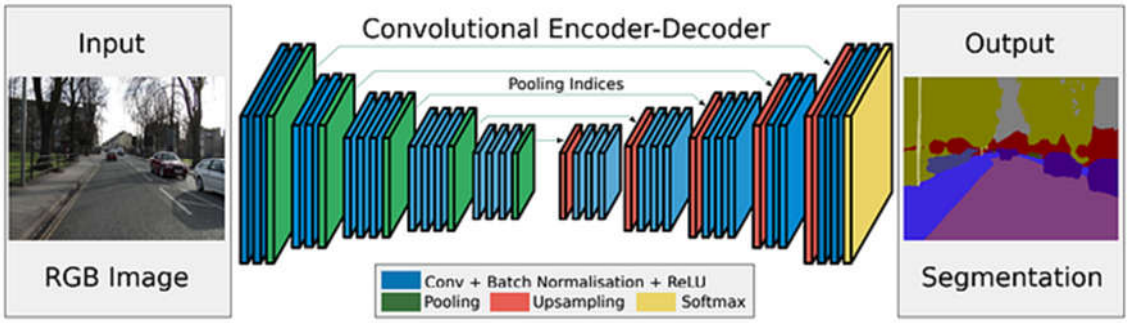

5.2. U-Net: U-Net is another popular architecture for semantic segmentation. It consists of a contracting path to capture context and an expansive path for precise localization. The skip connections between the encoder and decoder help maintain spatial information.

5.3. ENet (Efficient Neural Network):ENet is designed for real-time semantic segmentation. It is computationally efficient and suitable for applications with limited computational resources.

5.4. CRF (Conditional Random Field): Often used in combination with deep learning models, CRFs are used for post-processing the segmentation results. They help refine boundaries and remove artefacts in the output.

These are just a few of the methods used in computer vision for semantic segmentation. The choice of method depends on the specific task, computational resources, and the quality of segmentation required. Researchers continue to develop and refine these methods to improve

the accuracy and efficiency of semantic segmentation in various applications, such as autonomous driving, medical image analysis, and more.

5.5. TL-ESMNet

The TL-ESMNet framework integrates transfer learning with a dynamic ensemble-based segmentation model to tackle complex image segmentation tasks. It leverages pre-trained architectures like ResNet and VGG16 to capture powerful feature representations, which are essential for accurate segmentation. By incorporating spatial and channel attention mechanisms, the system actively emphasizes the most relevant regions and feature channels making it especially effective on small, low-contrast, or irregularly shaped structures. Within the ESM-Net stage, it employs multi-scale segmentation backbones (e.g., U-Net and DeepLabV3), then intelligently fuses their outputs based on image characteristics. This results in a robust and adaptive model that excels across diverse image conditions

5.6. Fully Convolutional Networks (FCN).

Fully Convolutional Networks (FCN) are a type of neural network architecture that is primarily used for image processing tasks. Unlike traditional Convolutional Neural Networks (CNNs), FCNs are designed to preserve the spatial information of the input data. This is achieved by replacing the fully connected layers in traditional CNNs with convolutional layers, allowing the network to output a probability map or a segmented image.

How FCN differs from traditional CNNs

The main difference between FCN and traditional CNNs lies in their architecture. Traditional CNNs typically consist of convolutional layers followed by fully connected layers, which are used for classification or regression tasks. However, the fully connected layers in traditional CNNs can lead to a loss of spatial information, making them less effective for tasks that require pixel-level predictions.

5.7. DeepLab V3

DeepLabv3 is a Deep Neural Network (DNN) architecture for Semantic Segmentation Tasks. It uses Atrous (Dilated) Convolutions to control the receptive field and feature map resolutions without increasing the total number of parameters. Another main attribute is something called Atrous Spatial Pyramid Pooling which effectively extracts multi-scale features that contain useful information for segmentation. In general, the network is able to capture dense feature maps with rich long-range information that can be used to accurately segment images.

5.8. Mask R-CNN

R-CNN, which stands for Region-based Convolutional Neural Network, is a type of deep learning model used for object detection in computer vision tasks. The term "R-CNN" actually refers to a family of models that share a common approach to object detection. The key idea behind R-CNN is to divide the object detection task into two stages: region proposal and object classification.

Region Proposal Network (RPN): Fast R-CNN integrates the region proposal step directly into the model. Instead of using an external method (as in the original R-CNN), it employs a Region Proposal Network to generate potential bounding boxes for objects within the image.

RoI Pooling: After obtaining region proposals, Fast R-CNN uses RoI pooling to extract fixed-size feature maps from the convolutional feature maps. This ensures that the extracted features are consistently sized, regardless of the size or aspect ratio of the original region proposals.

The integration of the region proposal step into the model, along with the use of RoI pooling, makes Fast R-CNN more computationally efficient as compared to the original R-CNN. The single-stage training and inference process also contributes to faster training and better overall performance. However, despite its improvements, Fast R-CNN still has room for optimization in terms of speed.

6. Contribution.

Proposed Flow of Work

Step 1. Data Collection. Eye Disease Retinal Images Data have been collected from [56]
Step 2. The dataset containing relevant information for the prediction of disease of Retinal Images have been taken.
Step 3. The data have been entered accurately and completely.
Step 4. Data Pre-processing: Cleaning of data and Removal of Outlier have been done.
Step 5. Taking care of missing data by input certain concerned data or removal of that data based on the nature and quantity of missing values.
Step 6. Cleaning the data by tackling inconsistencies, errors, and anomalies.
Step 7. Detection and removal of outliers that may affect the analysis.
Step 8. Implementation of Segmentation Algorithms and Performance Evaluation:
Step 9. UnderSegmentation algorithms, SegNet(Novel Segmented Neural Network),TL-EsmNet(transfer learning with a dynamic ensemble-based segmentation), FCN(Fully Convolutional Networks), DeepLab(Deep Neural Network), UNet(U-shaped Network), DeepLearn(Deep Learning), KMeans Clustering, Mask-R-CNN(Region-based Convolutional Neural Network), ENet(Efficient neural network), CNN(Convolution Neural Network) and CRF(Conditional Random Fields)have been used.
Step 10. Train the classifiers using the pre-processed data.
Step 11. Evaluate the performance of each classifier using evaluation metrics like accuracy, precision, recall, and F1 score.
Step 12.Performance Evaluation based on mean, standard deviation, skewness, kurtosis, homogeneity, contrast, correlation and Energy.
Step 13. The instructions as given in step 10 and step 12 have been executed among five types of Retinal Image data. These types are Bulging eyes, cataracts, crossed eyes, Glaucoma and Uveitus.
Step 14. Evaluate each segmentation algorithm, based on the parameters as narrated in step 11 and step 12.
Step 15. Select a particular segmentation based on the result as obtained in step 14.

6.1. Segmentation.

6.2. Application of Segmentation algorithms under Deep Learning Models.

The application of Segmentation algorithms under Deep Learning Models has been applied on input data [56]. The application of machine learning models has been furnished in figure 2. These are SegNet(Novel Segmented Neural Network),TL-EsmNet(transfer learning with a dynamic ensemble-based segmentation), FCN(Fully Convolutional Networks), DeepLab (Deep Neural Network), UNet(U-shaped Network), DeepLearn(Deep Learning), KMeans Clustering, Mask-R-CNN(Region-based Convolutional Neural Network), ENet(Efficient neural network), CNN(Convolution Neural Network) and CRF(Conditional Random Fields).

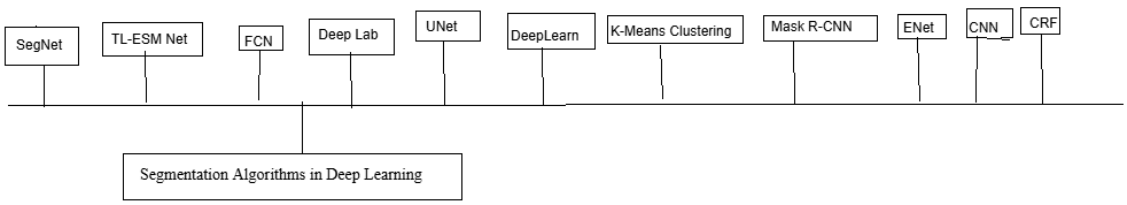

Figure 2: Deep Learning based Segmentation Algorithms(Flow Diagram)

Evaluate the performance of each segmentation algorithm using evaluation metrics like accuracy, precision, recall, and F1 score.
Performance Evaluation based on mean, standard deviation, skewness, kurtosis, homogeneity, contrast, correlation and Energy.
All the previous steps have been carried out in among five types of Retinal Image data. These types are Bulging eyes, cataracts, crossed eyes, Glaucoma and Uveitus.

6.3. Training and Test data.

The number of training date has been used as 70% and that of test data as 30% for the above models for better performance of the models.

7. Results.

The comparative study of all segmentation algorithms under deep learning on the basis of accuracy have been furnished in table 3 as furnished below. The comparative study of all segmentation algorithms under deep learning on the basis of mean retinal disease have been furnished in table 4. The comparative study of all segmentation algorithms under deep learning on the basis of standard deviation of retinal disease have been furnished in table 5.The comparative study of all segmentation algorithms under deep learning on the basis of skewness of retinal disease have been furnished in table 6. The comparative study of all segmentation algorithms under deep learning on the basis of kurtosis of retinal disease have been furnished in table 7. The comparative study of all segmentation algorithms under deep learning on the basis of homogeneity of retinal disease have been furnished in table 8. The comparative study of all segmentation algorithms under deep learning on the basis of contrast of retinal disease have been furnished in table 9. The comparative study of all segmentation algorithms under deep learning on the basis of correlation of retinal disease have been furnished in table 10. The comparative study of all segmentation algorithms under deep learning on the basis of energy of retinal disease have been furnished in table 11. The comparative study of all segmentation algorithms under deep learning on the basis of precision of retinal disease of type 0 have been furnished in table 12.The comparative study of all segmentation algorithms under deep learning on the basis of precision of retinal disease of type 1 have been furnished in table 13. The comparative study of all segmentation algorithms under deep learning on the basis of recall of retinal disease of type 0 have been furnished in table 14. The comparative study of all segmentation algorithms under deep learning on the basis of recall of retinal disease of type 1 have been furnished in table 15.The comparative study of all segmentation algorithms under deep learning on the basis of F1 score of retinal disease of type 0 have been furnished in table 16. The comparative study of all segmentation algorithms under deep learning on the basis of F1 score of retinal disease of type 1 have been furnished in table 17. The comparative study of all segmentation algorithms under deep learning on the basis of confusion matrix of retinal disease as bulging eyes have been furnished in table 18. The comparative study of all segmentation algorithms under deep learning on the basis of confusion matrix of retinal disease as cataracts have been furnished in table 19. The comparative study of all segmentation algorithms under deep learning on the basis of confusion matrix of retinal disease as crossed eyes have been furnished in table 20. The comparative study of all segmentation algorithms under deep learning on the basis of confusion matrix of retinal disease as glaucoma have been furnished in table 21. The comparative study of all segmentation algorithms under deep learning on the basis of confusion matrix of retinal disease as uveitus have been furnished in table 22. The Change of values of accuracy based on segmentation algorithms using retinal disease type has been furnished in figure 3. The Change of values of mean based on segmentation algorithms using retinal disease type has been furnished in figure 4.The Change of values of standard deviation based on segmentation algorithms using retinal disease type has been furnished in figure 5. The Change of values of skewness based on segmentation

algorithms using retinal disease type has been furnished in figure 6. The Change of values of kurtosis based on segmentation algorithms using retinal disease type has been furnished in figure 7. The Change of values of homogeneity based on segmentation algorithms using retinal disease type has been furnished in figure 8. The Change of values of contrast based on segmentation algorithms using retinal disease type has been furnished in figure 9. The Change of values of correlation based on segmentation algorithms using retinal disease type has been furnished in figure 10. The Change of values of energy based on segmentation algorithms using retinal disease type has been furnished in figure 11. The Change of values of precision based on segmentation algorithms using retinal disease type 0 has been furnished in figure 12. The Change of values of precision based on segmentation algorithms using retinal disease type 1 has been furnished in figure 13. The Change of values of recall based on segmentation algorithms using retinal disease type 0 has been furnished in figure 14. The Change of values of recall based on segmentation algorithms using retinal disease type 1 has been furnished in figure 15. The Change of values of F1 score based on segmentation algorithms using retinal disease type 0 has been furnished in figure 16. The Change of values of F1 score based on segmentation algorithms using retinal disease type 1 has been furnished in figure 17. The Change of values of confusion matrix based on segmentation algorithms using retinal disease type as bulging eyes has been furnished in figure 18. The Change of values of confusion matrixbased on segmentation algorithms using retinal disease type as cataracts has been furnished in figure 19. The Change of values of confusion matrix based on segmentation algorithms using retinal disease type as crossed eyes has been furnished in figure 20. The Change of values of confusion matrix based on segmentation algorithms using retinal disease type as glaucoma has been furnished in figure 21. The Change of values of confusion matrix based on segmentation algorithms using retinal disease type as uveitus has been furnished in figure 22.

Table 3
Segmentation algorithm versus AccuracyRetinal Disease Type wise

No	Segmentation Algorithm	Accuracy Bulging Eyes %	Accuracy Cataracts Eyes %	Accuracy Crossed Eyes %	Accuracy Glaucoma Eyes %	Accuracy Uveitus Eyes %
1	SegNet	55	34.4	19.9	11.3	13.18
2	Tel-ESM Net	82.69	13.86	83.15	10.17	85.36
3	FCN	43.66	63.2	13.9	92.7	0.117
4	Deep Lab	83.75	86.29	83.15	90.49	86.81
5	U Net	85.56	85.16	18.26	89.77	30.96
6	Deep Learn	85.72	86.29	83.15	90.49	86.81
7	KMeans Clustering	44.7	53.37	18.92	30.83	81.77
8	Mask R-CNN	29	16.6	23.05	39.52	15.43
9	E Net	52.6	84.12	73.82	90.44	85.65
10	CNN	55	46.04	73.83	90.44	85.64
11	CRF	55.29	46.03	81.08	68.94	82.59

Table 4
Segmentation algorithm versus Mean Retinal Disease Type wise

No	Segmentation Algorithm	Mean Bulging Eyes %	Mean Cataracts Eyes %	Mean Crossed Eyes %	Mean Glaucoma Eyes %	Mean Uveitus Eyes %
1	SegNet	161.96	56.96	238.27	188.16	134.04
2	Tel-ESM Net	116.09	120.29	238.27	188.16	136.04
3	FCN	123.01	127.48	161.82	238.98	136.04
4	Deep Lab	123.01	120.29	238.27	188.16	136.04
5	U Net	116.09	120.29	238.27	188.16	136.04
6	Deep Learn	116.09	120.29	238.27	188.16	136.05
7	KMeans Clustering	116.09	120.29	238.27	188.16	136.04
8	Mask R-CNN	116.09	120.29	238.27	188.16	136.04
9	E Net	116.09	120.29	238.27	188.16	218.56
10	CNN	116.09	120.29	238.27	188.16	218.56
11	CRF	116.09	120.29	238.27	188.16	136.04

Table 5
Segmentation algorithm versus Standard Deviation Retinal Disease Type wise

No	Segmentation Algorithm	Standard Deviation Bulging Eyes %	Standard Deviation Cataracts Eyes %	Standard Deviation Crossed Eyes %	Standard Deviation Glaucoma Eyes %	Standard Deviation Uveitus Eyes %
1	SegNet	39.05	38.06	30.56	45.43	36.24
2	Tel-ESM Net	56.51	34.78	30.57	45.42	36.24
3	FCN	29.37	46.59	23.14	35.84	36.24
4	Deep Lab	29.37	34.78	30.57	45.42	36.24
5	U Net	56.51	34.78	30.57	45.42	36.24
6	Deep Learn	56.51	34.78	30.57	45.43	36.24
7	KMeans Clustering	56.51	34.78	30.57	45.43	36.24
8	Mask R-CNN	56.51	34.78	30.57	45.43	36.24
9	E Net	56.51	34.78	30.57	45.43	41.68
10	CNN	56.51	34.78	30.57	45.43	41.68
11	CRF	56.51	34.78	30.57	45.43	36.24

Table 6
Segmentation algorithm versus Skewness of Retinal Disease Type wise

No	Segmentation Algorithm	Skewness Bulging Eyes %	Skewness Cataracts Eyes %	Skewness Crossed Eyes %	Skewness Glaucoma Eyes %	SkewnessUveitus Eyes %
1	SegNet	-1.24	3.05	-2.95	-0.99	-0.11
2	Tel-ESM Net	-0.07	-0.39	-2.95	-0.99	-0.12
3	FCN	-0.76	0.17	-0.27	-2.84	-0.12
4	Deep Lab	-0.76	-0.39	-2.95	-0.99	-0.12
5	U Net	-0.07	-0.39	-2.95	-0.99	-0.12

6	Deep Learn	-0.07	-0.39	-2.95	-0.99	-0.12
7	KMeans Clustering	-0.07	-0.39	-2.95	-0.99	-0.12
8	Mask R-CNN	-0.07	-0.39	-2.95	-0.99	-0.116
9	E Net	-0.07	-0.39	-2.95	-0.99	-1.92
10	CNN	-0.07	-0.39	-2.95	-0.99	-1.92
11	CRF	-0.07	-0.39	-2.95	-0.99	-0.116

Table 7
Segmentation algorithm versus Kurtosis of Retinal Disease Type wise

No	Segmentation Algorithm	Kurtosis Bulging Eyes %	Kurtosis Cataracts Eyes %	Kurtosis Crossed Eyes %	Kurtosis Glaucoma Eyes %	KurtosisUveitus Eyes %
1	SegNet	**-1.24**	**3.05**	**-2.95**	**-0.99**	-0.11
2	Tel-ESM Net	-0.07	-0.39	-2.95	-0.99	-0.12
3	FCN	-0.76	0.17	-0.27	-2.84	-0.12
4	Deep Lab	-0.76	-0.39	-2.95	-0.99	-0.12
5	U Net	-0.07	-0.39	-2.95	-0.99	-0.12
6	Deep Learn	-0.07	-0.39	-2.95	-0.99	-0.12
7	KMeans Clustering	-0.07	-0.39	-2.95	-0.99	-0.12
8	Mask R-CNN	-0.07	-0.39	-2.95	-0.99	-0.12
9	E Net	-0.07	-0.39	-2.95	-0.99	**-1.92**
10	CNN	-0.07	-0.39	-2.95	-0.99	**-1.92**
11	CRF	-0.07	-0.39	-2.95	-0.99	-0.12

Table 8
Segmentation algorithm versus Homogeneity of Retinal Disease Type wise

No	Segmentation Algorithm	Homogeneity Bulging Eyes %	Homogeneity Cataracts Eyes %	Homogeneity Crossed Eyes %	Homogeneity Glaucoma	Homogeneity Uveitus Eyes %
1	SegNet	0.269	0.257	0.888	0.557	0.287
2	Tel-ESM Net	0.225	0.155	0.888	0.557	0.287
3	FCN	0.417	0.291	0.348	0.629	0.287
4	Deep Lab	0.417	0.155	0.888	0.557	0.287
5	U Net	0.225	0.155	0.888	0.557	0.287
6	Deep Learn	0.225	0.155	0.888	0.557	0.287
7	KMeans Clustering	0.225	0.155	0.888	0.557	0.287
8	Mask R-CNN	0.225	0.155	0.888	0.557	0.287
9	E Net	0.225	0.155	0.888	0.557	0.545

10	CNN	0.225	0.155	0.888	0.557	0.287
11	CRF	0.225	0.155	0.888	0.557	0.287

Table 9
Segmentation algorithm versus Contrast of Retinal Disease Type wise

No	Segmentation Algorithm	Contrast Bulging Eyes %	Contrast Cataracts Eyes %	Contrast Crossed Eyes %	Contrast Glaucoma	Contrast Uveitus Eyes %
1	SegNet	269.17	**108.84**	526.49	457.41	73.33
2	Tel-ESM Net	288.22	149.41	526.49	457.41	73.33
3	FCN	**74.69**	247.28	**249.47**	**423.90**	**73.33**
4	Deep Lab	74.69	149.41	526.49	457.41	73.33
5	U Net	288.22	149.41	526.49	457.41	73.33
6	Deep Learn	288.22	149.41	526.49	457.41	73.33
7	KMeans Clustering	288.22	149.41	526.49	457.41	73.33
8	Mask R-CNN	288.22	149.41	526.49	457.41	73.33
9	E Net	288.22	149.41	526.49	457.41	73.33
10	CNN	288.22	149.41	526.49	457.41	425.54
11	CRF	288.22	149.41	526.49	457.41	73.33

Table 10
Segmentation algorithm versus Correlation of Retinal Disease Type wise

No	Segmentation Algorithm	Correlation Bulging Eyes %	Correlation Cataracts Eyes %	Correlation Crossed Eyes %	Correlation Glaucoma	Correlation Uveitus Eyes %
1	SegNet	0.97	0.98	0.664	0.89	0.96
2	Tel-ESM Net	0.96	0.966	0.664	0.89	0.96
3	FCN	0.987	0.975	0.967	0.915	0.962
4	Deep Lab	0.987	0.966	0.664	0.891	0.962
5	U Net	0.96	0.966	0.664	0.89	0.96
6	Deep Learn	0.96	0.966	0.664	0.89	0.96
7	KMeans Clustering	0.96	0.966	0.664	0.89	0.96
8	Mask R-CNN	0.96	0.966	0.664	0.89	0.96
9	E Net	0.96	0.966	0.664	0.89	0.89
10	CNN	0.96	0.966	0.664	0.89	0.89
11	CRF	0.96	0.966	0.664	0.89	0.96

Table 11
Segmentation algorithm versus Energy of Retinal Disease Type wise

No	Segmentation Algorithm	Energy Bulging Eyes %	Energy Cataracts Eyes %	Energy Crossed Eyes %	Energy Glaucoma	Energy Uveitus Eyes %
1	SegNet	0.049	0.019	0.716	0.439	0.029
2	Tel-ESM Net	0.022	0.015	0.717	0.439	0.029
3	FCN	0.034	0.029	0.069	0.534	0.029
4	Deep Lab	0.034	0.015	0.717	0.439	0.029
5	U Net	0.022	0.015	0.717	0.439	0.029
6	Deep Learn	0.022	0.015	0.717	0.439	0.029
7	KMeans Clustering	0.022	0.015	0.717	0.439	0.029
8	Mask R-CNN	0.022	0.015	0.717	0.439	0.337
9	E Net	0.022	0.015	0.717	0.439	0.337
10	CNN	0.022	0.015	0.717	0.439	0.337
11	CRF	0.022	0.015	0.717	0.439	0.029

Table 12
Segmentation algorithm versus Precision of Retinal Disease Type wise of Type 0

No	Segmentation Algorithm	Precision Bulging Eyes	Precision Cataracts Eyes	Precision Crossed Eyes	PrecisionGlaucoma eyes	PrecisionUveitus Eyes
1	SegNet	0.8	0.82	0.94	1.00	0
2	Tel-ESM Net	0.86	1.00	0.83	1.00	0.87
3	FCN	1.00	0.81	0.15	0.93	1.00
4	Deep Lab	0.84	0.86	0.83	0.9	0.87
5	U Net	0.86	0.86	0.82	0.9	0.92
6	Deep Learn	0.86	0.86	0.83	0.9	0.87
7	KMeans Clustering	0.86	0.93	0.76	0.89	0.98
8	Mask R-CNN	0.91	1.00	1.00	0.93	1.0
9	E Net	0.94	0.86	0.87	0.9	0.86
10	CNN	0.85	0.80	0.87	0.9	0.86
11	CRF	0.85	0.8	0.83	0.91	0.98

Table 13
Segmentation algorithm versus Precision of Retinal Disease Type wise of Type 1

No	Segmentation Algorithm	Precision	Precision	Precision	PrecisionGlaucoma eyes	PrecisionUveitus Eyes

		Bulging Eyes	Cataracts Eyes	Crossed Eyes		
1	SegNet	0.03	0.11	0.17	0.1	0.13
2	Tel-ESM Net	0.09	0	1	0.1	0.29
3	FCN	0	0	0	0	0
4	Deep Lab	0	0	0	0	0
5	U Net	0	0	0.17	0	0.15
6	Deep Learn	0	0	0	0	0
7	KMeans Clustering	0.15	0.19	0.17	0.09	0.41
8	Mask R-CNN	0.15	0.14	0.,18	0.11	0.13
9	E Net	**0.21**	0.03	0.31	0.04	0
10	CNN	0.14	0.07	0.31	0.04	0
11	CRF	0.14	0.07	0.24	0.11	0.42

Table 14
Segmentation algorithm versus Recall of Retinal Disease Type wise of Type 0

No	Segmentation Algorithm	Precision Bulging Eyes	Precision Cataracts Eyes	Precision Crossed Eyes	PrecisionGlaucoma eyes	PrecisionUveitus Eyes
1	SegNet	0.63	0.31	0.04	0.02	0
2	Tel-ESM Net	0.96	0	1.00	0.01	0.97
3	FCN	0.52	0.75	0.15	1.0	0
4	Deep Lab	1.0	1.0	1.0	1.0	1.0
5	U Net	1.0	0.99	0.02	0.99	0.22
6	Deep Learn	1.0	1.0	1.0	1.0	1.0
7	KMeans Clustering	0.42	0.50	0.04	0.27	0.81
8	Mask R-CNN	0.19	0.03	0.07	0.36	0.03
9	E Net	0.48	0.97	0.8	1.0	1.0
10	CNN	0.58	0.49	0.87	1.0	1.0
11	CRF	0.58	0.49	0.96	0.73	0.82

Table 15
Segmentation algorithm versus Recall of Retinal Disease Type wise of Type 1

No	Segmentation Algorithm	Precision Bulging Eyes	Precision Cataracts Eyes	Precision Crossed Eyes	PrecisionGlaucoma eyes	PrecisionUveitus Eyes
1	SegNet	0.07	0.54	0.99	1.00	1.00

2	Tel-ESM Net	0.02	1.0	0	1.00	0.07
3	FCN	0	0	0	0	0
4	Deep Lab	0	0	0	0	0
5	U Net	0	0	0.98	0	0.87
6	Deep Learn	0	0	0	0	0
7	KMeans Clustering	0.6	0.76	0.94	0.68	0.87
8	Mask R-CNN	0.88	1.00	1.00	0.75	1.00
9	E Net	0.82	0	0.44	0	0
10	CNN	0.4	0.24	0.44	0	0
11	CRF	0.4	0.24	0.06	0.32	0.87

Table 16
Segmentation algorithm versus F1 Score of Retinal Disease Type wise of Type 0

No	Segmentation Algorithm	Precision Bulging Eyes	Precision Cataracts Eyes	Precision Crossed Eyes	PrecisionGlaucoma eyes	PrecisionUveitus Eyes
1	SegNet	0.71	0.45	0.08	0.04	0
2	Tel-ESM Net	0.90	0.91	**0.91**	0.01	0.92
3	FCN	0.69	0.78	0.27	0.96	0
4	Deep Lab	0.91	0.93	0.91	0.95	0.93
5	U Net	0.92	0.92	0.04	0.95	0.36
6	Deep Learn	0.92	0.93	0.91	0.95	0.93
7	KMeans Clustering	0.57	0.65	0.07	0.41	0.89
8	Mask R-CNN	0.32	0.07	0.14	0.52	0.05
9	E Net	0.63	0.91	0.84	0.95	0.92
10	CNN	0.69	0.61	0.84	0.95	0.92
11	CRF	0.69	0.61	0.89	0.81	0.89

Table 17
Segmentation algorithm versus F1 Score of Retinal Disease Type wise of Type 1

No	Segmentation Algorithm	Precision Bulging Eyes	Precision Cataracts Eyes	Precision Crossed Eyes	PrecisionGlaucoma eyes	PrecisionUveitus Eyes
1	SegNet	0.04	0.18	0.29	0.18	0.23
2	Tel-ESM Net	0.04	0.24	0	0.17	0.12

3	FCN	0	0	0	0	0
4	Deep Lab	0	0	0	0	0
5	U Net	0	0	0.29	0	0.25
6	Deep Learn	0	0	0	0	0
7	KMeans Clustering	0.24	0.31	0.28	0.16	0.56
8	Mask R-CNN	0.26	0.25	0.3	0.19	0.24
9	E Net	0.33	0.01	0.36	0	0
10	CNN	0.20	0.11	0.44	0	0
11	CRF	0.20	0.11	0.09	0.16	0.57

Table 18
Confusion Matrix of Bulging Eyes based onSegmentation algorithm

No	Segmentation Algorithm	True Positive	False Positive	False Negative	True Negative
1	SegNet	25,357	14,768	6,150	475
2	Tel-ESM Net	41,590	1,702	7,038	175
3	FCN	21,962	0	0	0
4	Deep Lab	42,128	0	8,173	0
5	U Net	43,215	77	7,213	0
6	Deep Learn	43,292	0	7,213	0
7	KMeans Clustering	18,277	25,015	2,910	4,303
8	Mask R-CNN	8,318	34,974	871	6,342
9	E Net	20,654	22,638	1,287	5,926
10	CNN	25,015	18,277	4,303	2,910
11	CRF	25,015	18,277	4,303	2,910

Table 19
Confusion Matrix of Cataracts based onSegmentation algorithm

No	Segmentation Algorithm	True Positive	False Positive	False Negative	True Negative
1	SegNet	13,746	29,949	3,057	3,568
2	Tel-ESM Net	49,932	0	8,497	0
3	FCN	5,362	0	1,224	0
4	Deep Lab	43,542	0	6,921	0
5	U Net	42,978	564	6,921	0
6	Deep Learn	43,542	0	6,921	0
7	KMeans Clustering	21,652	21,889	1,639	5,282
8	Mask R-CNN	1,463	42,079	0	6,921
9	E Net	42,415	1,127	6,889	32
10	CNN	21,550	21,992	5,239	1682

11	CRF	21,550	21,992	5,239	1682

Table 20
Confusion Matrix of Crossed Eye based onSegmentation algorithm

No	Segmentation Algorithm	True Positive	False Positive	False Negative	True Negative
1	SegNet	1,684	40,248	100	8,397
2	Tel-ESM Net	49,932	0	8,487	0
3	FCN	6,997	**0**	**0**	0
4	Deep Lab	41,932	0	8497	0
5	U Net	903	41,029	192	8,305
6	Deep Learn	43,542	0	6,921	0
7	KMeans Clustering	1518	40,414	476	8,021
8	Mask R-CNN	3,129	38,803	0	8,497
9	E Net	33,531	8,401	4,797	3,700
10	CNN	33,531	8,401	4,797	3,700
11	CRF	40,414	1,518	8,021	476

Table 21
Confusion Matrix of Glaucoma based onSegmentation algorithm

No	Segmentation Algorithm	True Positive	False Positive	False Negative	True Negative
1	SegNet	924	44,543	0	4,777
2	Tel-ESM Net	334	45,133	0	4,777
3	FCN	46,695	0	3,625	0
4	Deep Lab	45,467	0	4,777	0
5	U Net	45,106	361	4,777	0
6	Deep Learn	41,932	0	8,497	0
7	KMeans Clustering	12,226	33,241	1,541	3,263
8	Mask R-CNN	16,254	29,213	1,173	3604
9	E Net	45,442	25	4,776	1
10	CNN	45,442	25	4,776	1
11	CRF	40,414	1,518	5,021	476

Table 22
Confusion Matrix of Uveitus based on Segmentation algorithm

No	Segmentation Algorithm	True Positive	False Positive	False Negative	True Negative
1	SegNet	0	43,607	0	6,625

2	Tel-ESM Net	42,399	1,208	6,142	483
3	FCN	59	43,548	0	6,625
4	Deep Lab	43,607	0	6,625	0
5	U Net	9,778	33,829	849	5,776
6	Deep Learn	43,607	0	6,625	0
7	KMeans Clustering	12,226	33,241	1,541	3,263
8	Mask R-CNN	1130	42,477	0	6,625
9	E Net	43,033	0	7,213	0
10	CNN	43,033	0	7,213	0
11	CRF	35,733	7,874	867	5,758

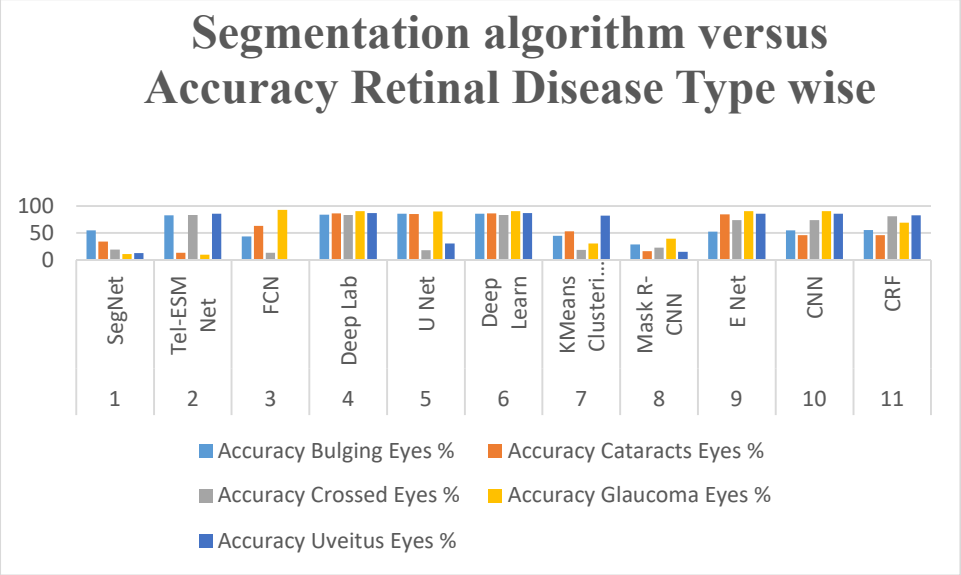

Figure 3: Segmentation Algorithm wise Accuracy

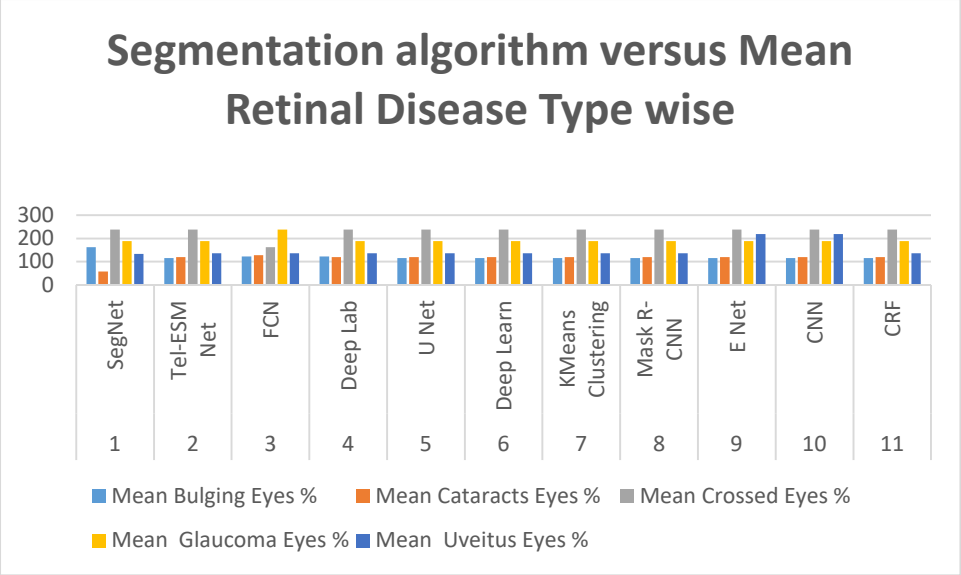

Figure 4: Segmentation Algorithm wise Mean

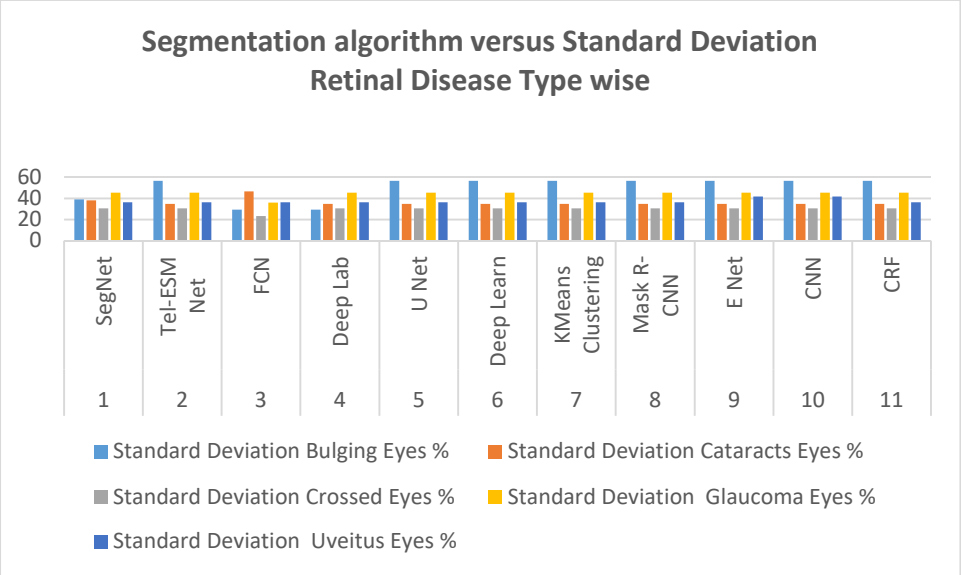

Figure 5: Segmentation Algorithm wise Standard Deviation

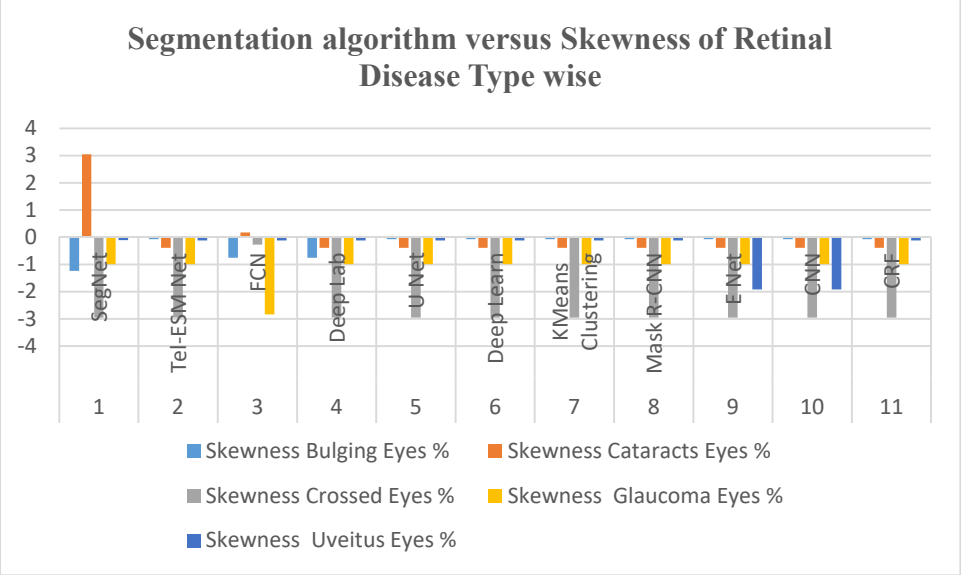

Figure 6: Segmentation Algorithm wise Skewness

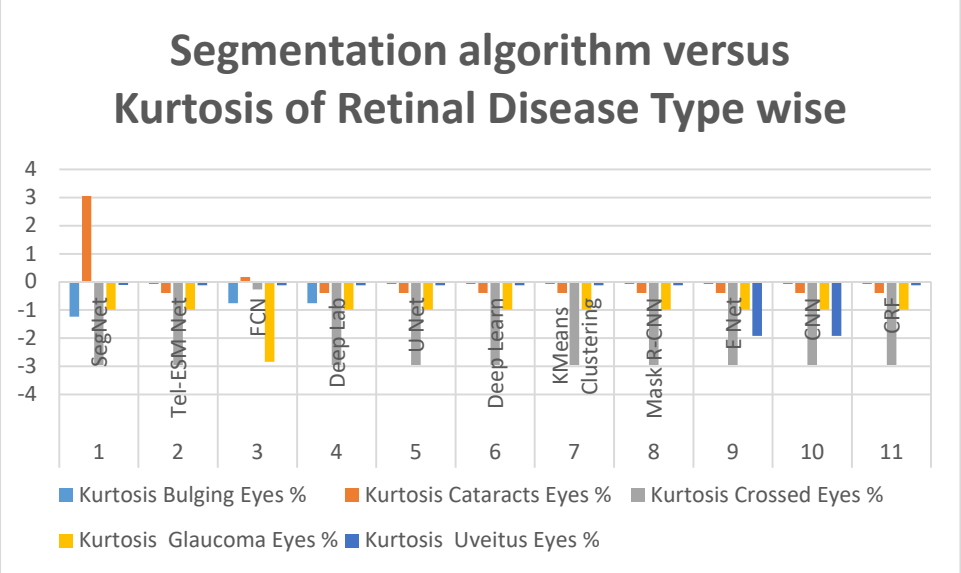

Figure 7: Segmentation Algorithm wise Kurtosis

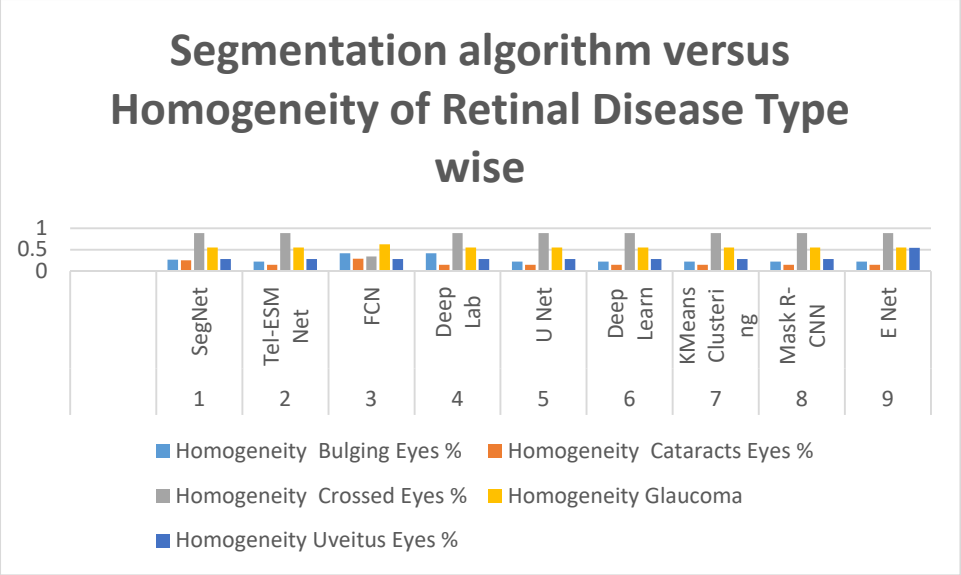

Figure 8: Segmentation Algorithm wise Homogeneity

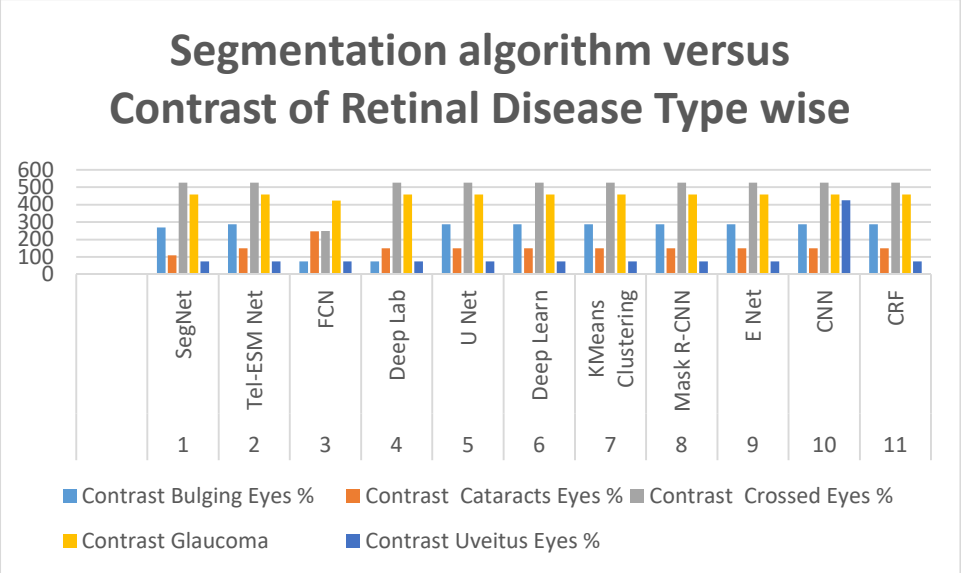

Figure 9: Segmentation Algorithm wise Contrast

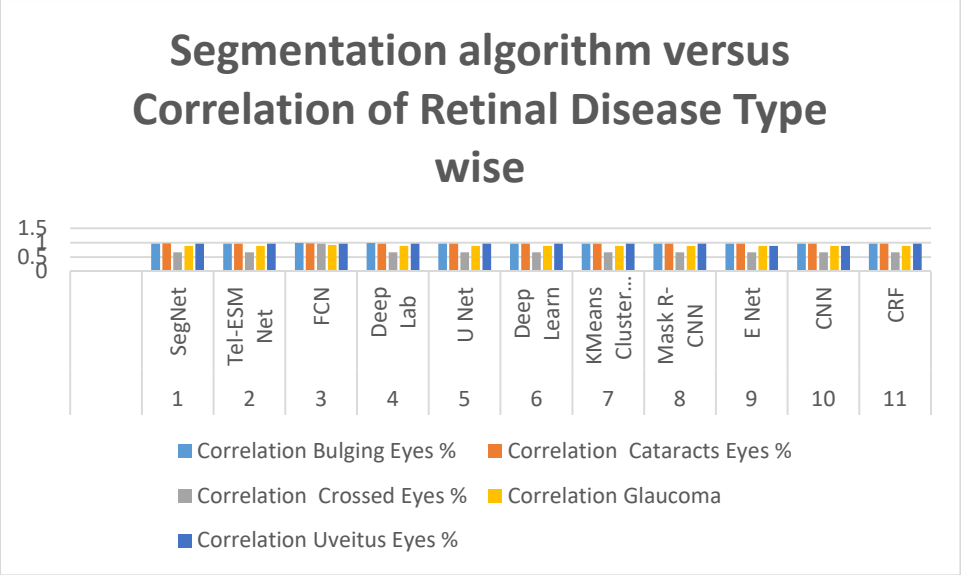

Figure 10: Segmentation Algorithm wise Correlation

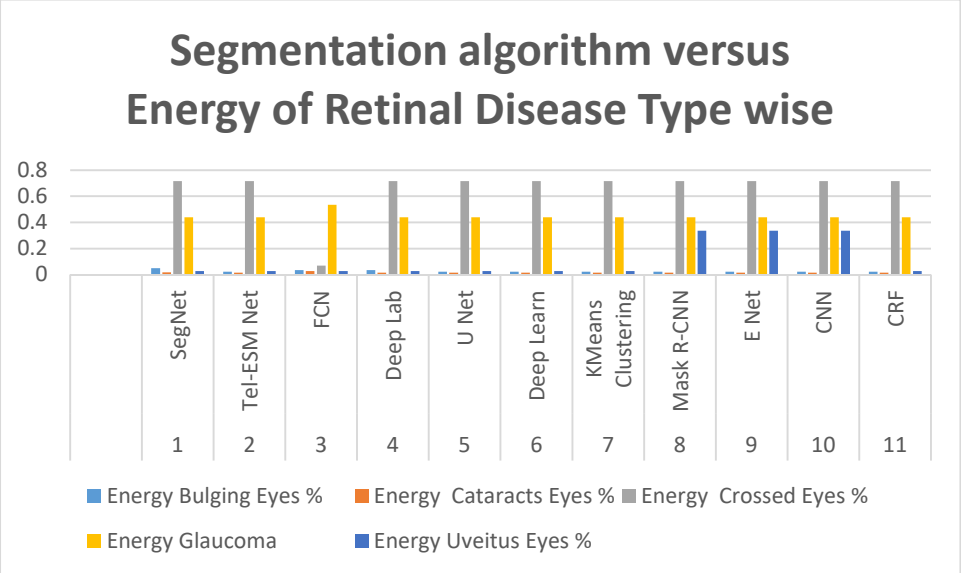

Figure 11: Segmentation Algorithm wise Energy

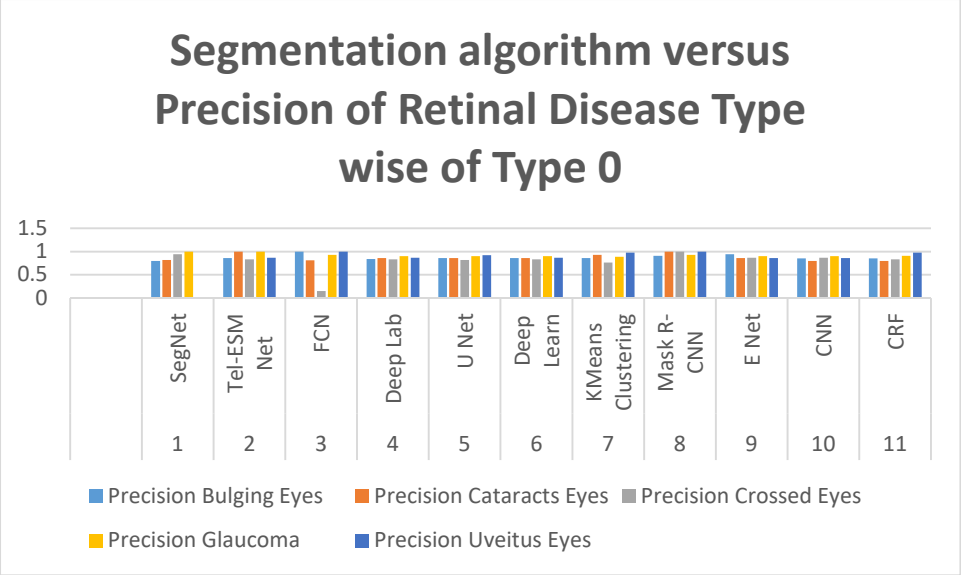

Figure 12: Segmentation Algorithm wise Precision of Type 0

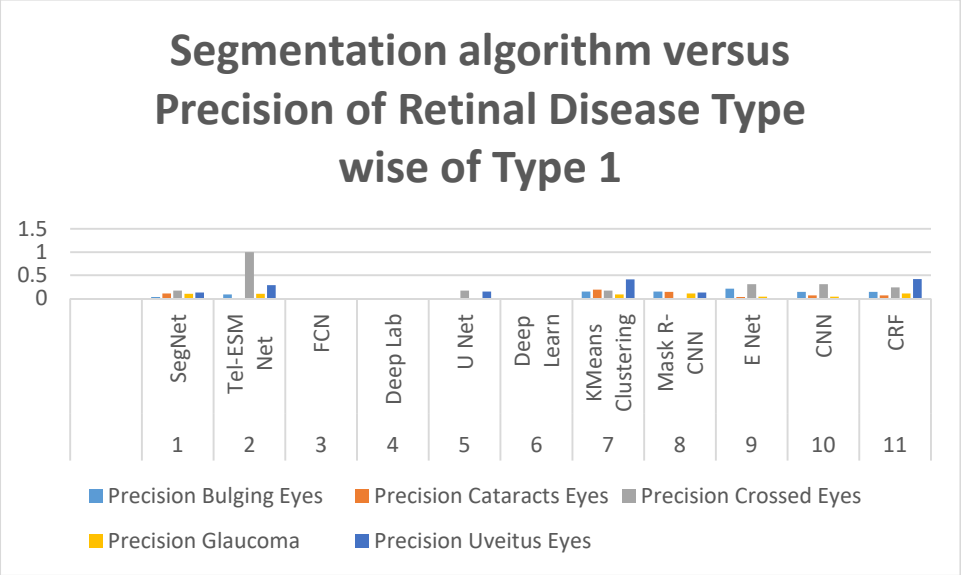

Figure 13: Segmentation Algorithm wise Precision of Type 1

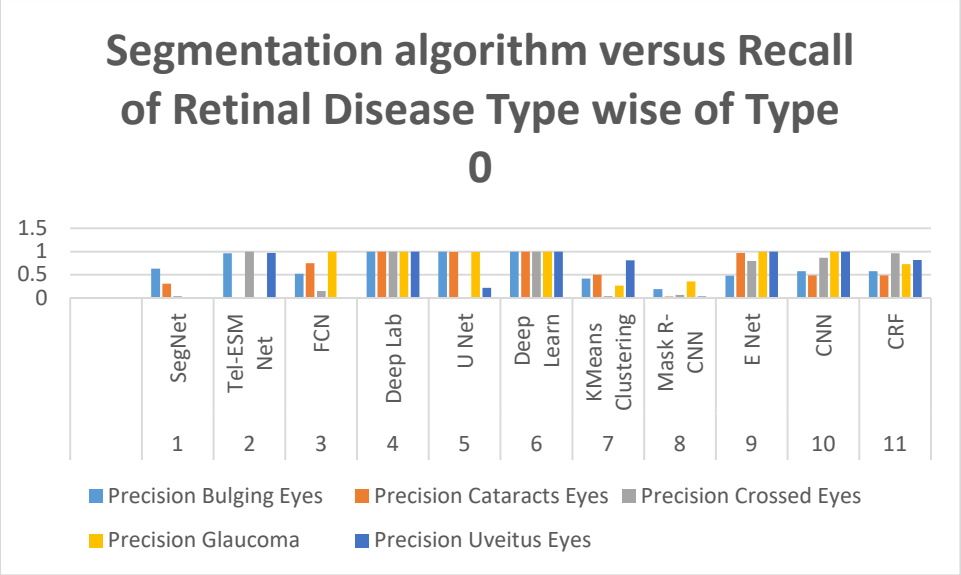

Figure 14: Segmentation Algorithm wise Recall of Type 0

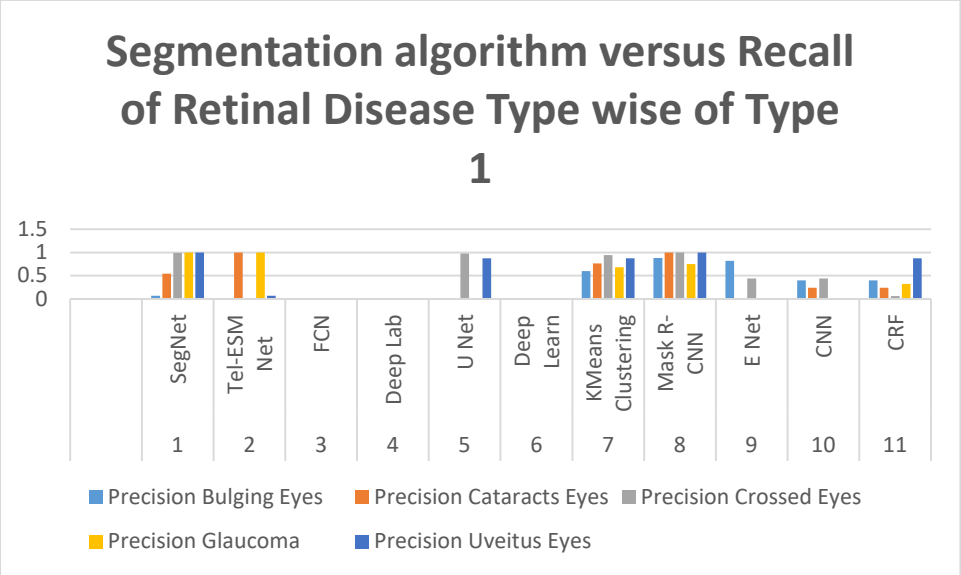

Figure 15: Segmentation Algorithm wise Recall of Type 1

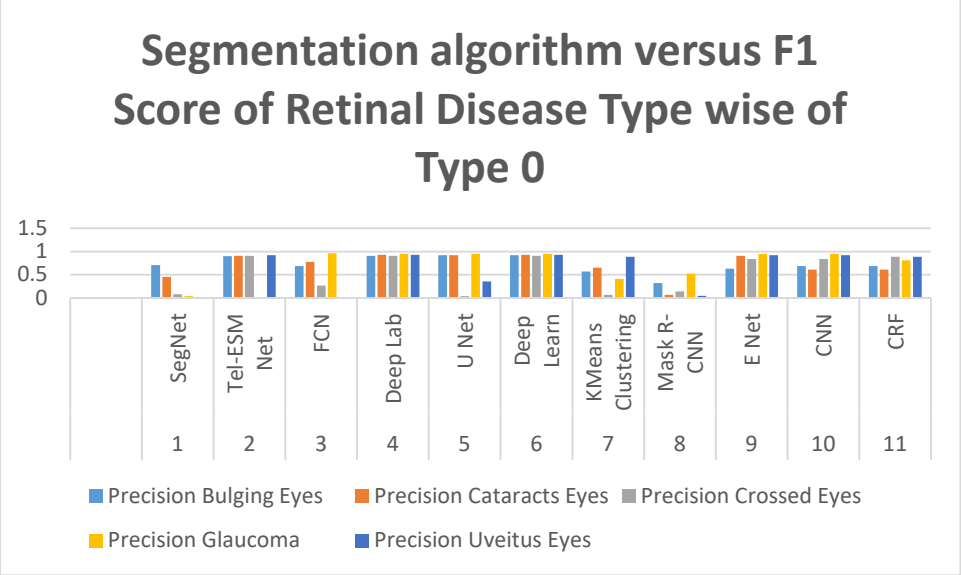

Figure 16: Segmentation Algorithm wise F1 Score of Type 0

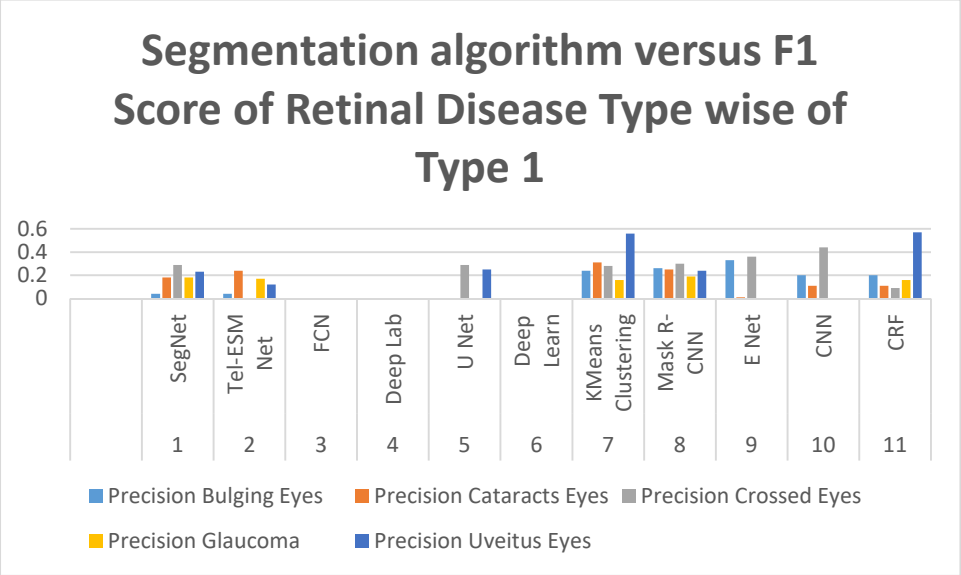

Figure 17: Segmentation Algorithm wise F1 Score of Type 1

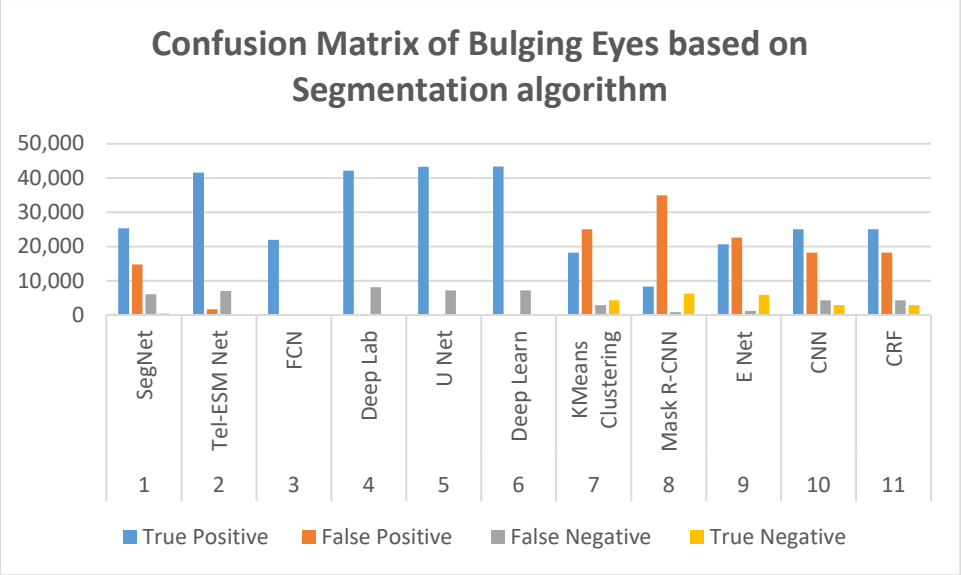

Figure 18: Segmentation Algorithm wise Confusion Matrix of Bulging Eyes

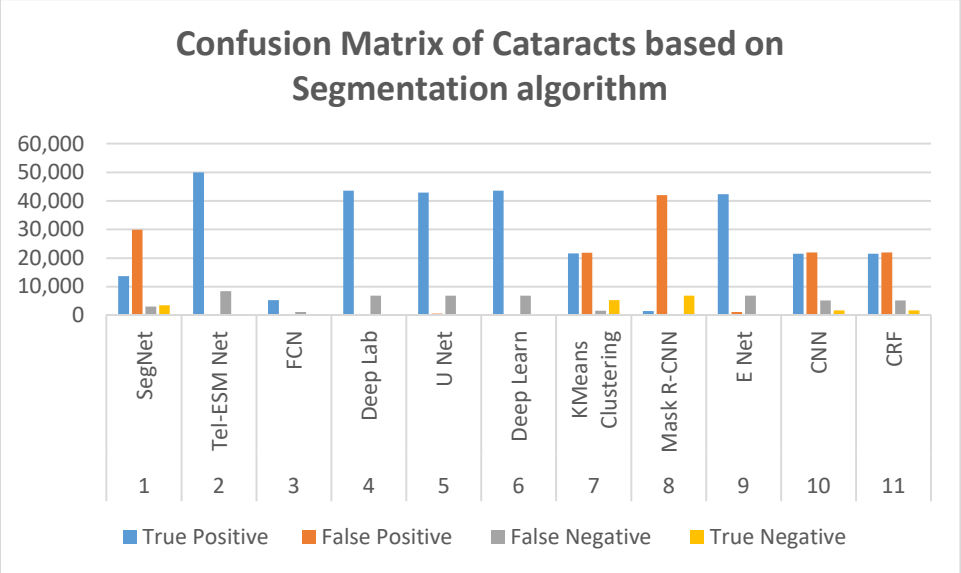

Figure 19: Segmentation Algorithm wise Confusion Matrix of Cataracts

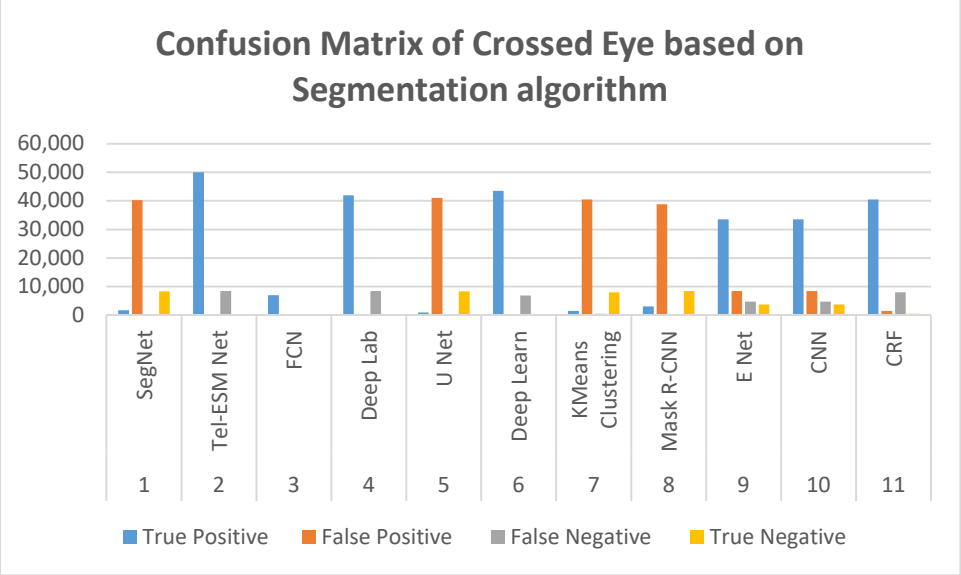

Figure 20: Segmentation Algorithm wise Confusion Matrix of Crossed Eye

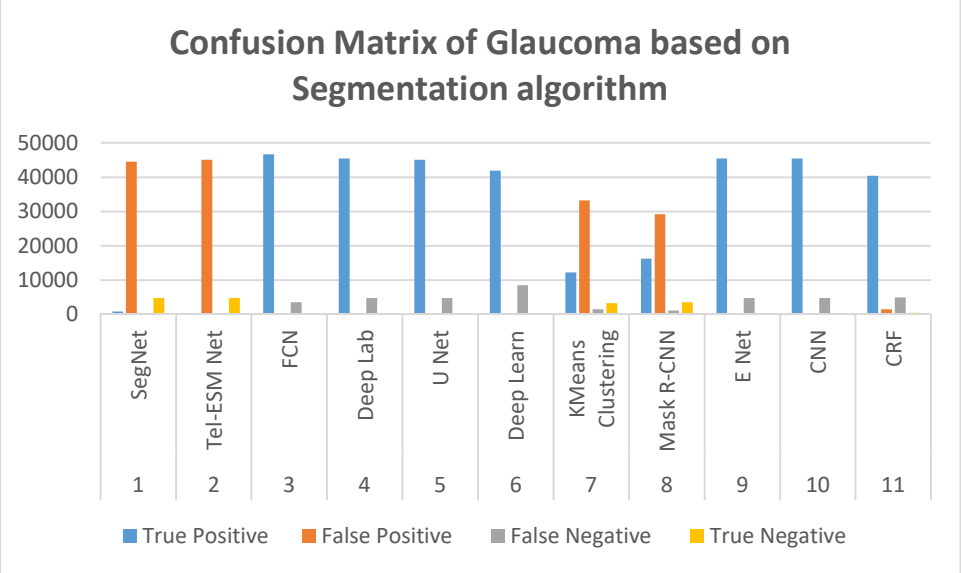

Figure 21: Segmentation Algorithm wise Confusion Matrix of Glaucoma

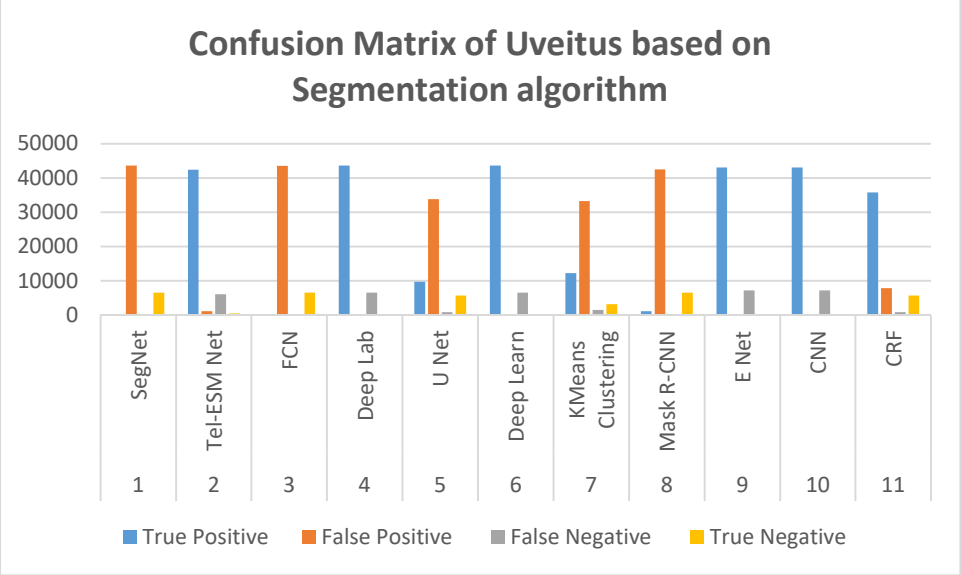

Figure 22: Segmentation Algorithm wise Confusion Matrix of Uveitus

8. Conclusion.

From table 3 based on accuracy, Deep Learning segment has been preferred in 4 cases and Tel-EsmNet in 1 case. From table 5, based on minimum standard deviation values, FCN(Fully Convolution Neural Network) has been preferred in 4 cases, Mask-R-CNN in 2 cases, K-Means clustering and CRF in 2 cases. From table 6 based on skewness(closer to zero), Tel-EsmNet has been preferred in 2 cases, FCN(Fully Convolution Neural Network), Deep Learning segment, K-Means clustering and Mask-R-CNN in 2 cases. Since the number of preferred cases is 2 in 5 models, no decision can be arrived based on data of table 5. From table 7 based on kurtosis(closer to 3), SegNet is preferred in 4 cases, ENet and CNN in 1 case. From table 8 based on homogeneity(more values are preferred), FCN(Fully Convolution Neural Network) has been preferred in 3 cases, Tel-ESM Net , UNet and CNN in 1 case. From table 9 based on contrast (less values are preferred), FCN(Fully Convolution Neural Network) has been preferred in 4 cases and SegNet in 1 case. From table 10 based on correlation (more values are preferred), FCN(Fully Convolution Neural Network) has been preferred in 4 cases and SegNet in 1 case. From table 11 based on energy (more values are preferred), FCN(Fully Convolution Neural Network) has been preferred in 2 cases and SegNet in 1 case. From table 12 of type 0 dataset, based on precision (more values are preferred), Mask-R-CNN has been preferred in 3 cases, Tel EsmNet and FCN in 2 cases. From table 13 of type 1 dataset, based on precision (more values are preferred), ENet and CRF have been preferred in 2 cases, CNN and K-means clustering in 1 case. From table 14 of type 0 dataset, based on recall (more values are preferred), Deep Learn(Deep Learning Segment) has been preferred in 5 cases, DeepLab in 3 cases, Enet and CNN in 2 cases. From table 15 of type 1 dataset, based on recall (more values are preferred), Mask-R-CNN has been preferred in 4 cases, Tel-EsmNet in 2 cases. From table 16 of type 0 dataset, based on F1 score (more values are preferred), Deep Learn(Deep Learning Segment) has been preferred in 5 cases, Tel-EsmNet in 1 case. From table 17 of type 1 dataset, based on F1 score (more values are preferred), Mask R CNN, CNN, CRF and K-means clustering in 1 case each. From table 18using data as bulging eyes based on confusion matrix (less values of false positive and false negatives are preferred), FCN(Fully Convolution Neural

Network) is preferred in 1 case. From table 20 using data as crossed eyes based on confusion matrix (less values of false positive and false negatives are preferred), FCN(Fully Convolution Neural Network) is preferred in 1 case. Table 19 of using data as cataracts, table 21of using data as glaucoma and table 22 of using data as uveitus does not arrive any decision since no concrete decision regarding confusion matrix (less values of false positive and false negatives are preferred) has been obtained. Since, Table 4 contains the mean of estimated values based on used models, no decision has been arrived.
A table named Table 23 indication the preference of segmentation model has been prepared which has been furnished. Finally, a summary table has been prepared indicating the selected segmentation model and the number cases preferred by the selected model.

Table 23
Selected Segmentation algorithm with reference to table no

no	Selected segmentation model	Count supported in table	Table no as reference
1	DeepLearn(Deep Learning Segment)	4	Table 4
2	DeepLearn(Deep Learning Segment)	5	Table 14
3	DeepLearn(Deep Learning Segment)	5	Table 16
4	FCN((Fully Convolution Neural Network)	4	Table 5
5	FCN((Fully Convolution Neural Network)	4	Table 9
6	FCN((Fully Convolution Neural Network)	4	Table 10
7	FCN((Fully Convolution Neural Network)	2	Table 11
8	FCN((Fully Convolution Neural Network)	1	Table 18
9	FCN((Fully Convolution Neural Network)	1	Table 20
10	Mask-R-CNN	3	Table 12
11	Mask-R-CNN	4	Table 15
12	Seg Net	4	Table 5

Table 24
Selected Segmentation algorithm with count supported

No	Selected segmentation model	Count Supported
1	DeepLearn(Deep Learning Segment)	3
2	**FCN((Fully Convolution Neural Network)**	**6**
3	Mask-R-CNN	2
4	Seg Net	1

From above discussion as furnished in table 23, it is evident that Deep Learn(Deep Learning Segment) has been preferred in 3 cases, namely from table 4, table 14 and table 16. FCN(Fully Convolution Neural Network) has been preferred in 6 cases, namely from table 5, table 9, table 10, table 11, table 18 and table 20. Mask R CNN has been preferred in 2 cases from table 12 and table 15. Therefore, all these, FCN(Fully Convolution Neural Network) is the selected segmentation algorithm for gathering of information eyes for the prediction of retinal disease as furnished in table 24. Further it can be mentioned that Fully Convolution Neural Network(FCN) has been chosen as the Best segmentation algorithms in prediction of retinal diseases.
The strength of FCN is furnished as follows :-
FCN has Dense pixel-wise output(FCNs directly produce a per-pixel segmentation map in a

single end-to-end forward pass),Flexible input resolution (They accept images of arbitrary size and output correspondingly-sized segmentation), Efficiency and speed
An FCN contains only convolutional layers, which enables it to take an image of arbitrary size and produce a segmentation map of the same size skip connections produce accurate and detailed segmentations.
Fully Convolutional Networks are powerful for segmentation because they can deliver dense, end-to-end pixel classification, support variable image sizes, preserve spatial details through skip connections and efficient up sampling, run fast and lean, suitable for real-time tasks
Their streamlined architecture remains the foundationof modern segmentation models like U-Net and DeepLab.

References

[1] P. Shobana, J. Deny, P. Swapna, "Automated Skin Lesion Segmentationthrough HarmonizingDermoscopic Imageswith Fusionbased White Balancing", Journal of Theoretical and Applied Information Technology, 15th May 2025. Vol.103. No.9, 3851-3865.
[2] AbujalamboMahmoud I M, NorAzlinahBinti MD Lazam, MalikJawarneh, Shadi M S Hilles, AbdallahAltrad, "Efficient MRI Segmentation OF SpineHemangiomas: A Novel Modified U-NET Approachto EnhanceTumor Boundary Detection", Journal of Theoretical and Applied Information Technology 31st March 2025. Vol.103. No.6. ISSN: 1992-8645. 2468-2478.
[3] JakkulaSravanthi, Banda VenkataRamana, JuthukaAruna Devi, SuragaliChanti, SradhanjaliPattanaik, PalthiyaAnantha Rao, MaradaSrinivasa Rao, "Deep Learning-Based Classification and Segmentation of Chest Pathologies", Journal of Theoretical and Applied Information Technology, 31st March 2025. Vol.103. No.6, ISSN: 1992-8645, 2562-2578.
[4] Satyanarayana Reddy Beram , R Lalchhanhima , and Ksh. Robert Singh, "Enhancing Breast Tumor Segmentation with TLESMNet: A Transfer Learning and Ensemble-Based Approach for Mammograms", Journal of Advances in Information Technology, Vol. 16, No. 6, 2025. doi: 10.12720/jait.16.6.838-853.
838-853.
[5] FarhaFatina Wahid , Raju G. , Shijo M. Joseph , Debabrata Swain , Om Prakash Das , and Biswaranjan Acharya ," A Novel Fuzzy-Based Thresholding Approach for Blood Vessel Segmentation from Fundus Image", Journal of Advances in Information Technology, Vol. 14, No. 2, 2023. doi: 10.12720/jait.14.2.185-192 , 185-192.
[6]Mandeep Kaur, "Plant Disease Image Segmentation applying the KMeans
Algorithm, Firefly, and Particle Swarm Optimisation", International Journal for Research in Applied Science & Engineering Technology (IJRASET**),** ISSN: 2321-9653; IC Value: 45.98; SJ Impact Factor: 7.538, Volume 11 Issue V May 2023, 982-990.
[7] Sri LasyaAvula, GajjalaAkshara, Mr. S. Sreehari, Dr. SVR. Manimala, "Efficient 3D Medical Image Segmentation using CoTr: Bridging CNN and Transformer", International Journal for Research in Applied Science & Engineering Technology (IJRASET**),** ISSN: 2321-9653; IC Value: 45.98; SJ Impact Factor: 7.538, Volume 11 Issue V May 2023, 4748-4759.
[8] K. Subha, B. Gokul, D. Kamal Navas, K. Yashwin, "Cross-Correlation Driven Aerial Image Segmentation: Leveraging Multi-Scale Features and Edge Information", International Journal for Research in Applied Science & Engineering Technology (IJRASET**)** ISSN: 2321-9653; IC Value: 45.98; SJ Impact Factor: 7.538 Volume 12 Issue V May 2024, 416-421.
[9] ShireenKausar, Dr.SuvarnaNandyal, "A Focused Study on Otsu's Thresholding for Segmenting Images of Paralysis-Affected Individuals", International Journal for Research in Applied Science & Engineering Technology (IJRASET) ISSN: 2321-9653; IC Value: 45.98; Volume 13 Issue VI June 2025, 1894-1900.

[10] D.Mahita, A.Sravya, Ch.Shireesha, M.Jhansi, Dr.P.M.K.Prasad, "Deep Learning Based Image Segmentation for Diagnosis of Spondylolis thesis from Lumbar Spine X-RAY", International Journal for Research in Applied Science & Engineering Technology (IJRASET) ISSN: 2321-9653; IC Value: 45.98; SJ Impact Factor: 7.538 Volume 13 Issue IV Apr 2025. 2107-2116.
[11] Dharavath Ramesh & Yogendra Singh Katheria, "Ensemble method based predictive model for analyzing disease datasets: a predictive analysis approach", Health and Technology, volume 9, 533-545, 2019.https://doi.org/10.1007/s12553-019-00299-3.
[12] R. Suresh & Nagaratna P. Hegde, "Intelligent Ensemble Algorithm for Feature Selection and Effective Prediction for Heart Disease Using SVM and KNN", Cognitive Science and Technology ((CSAT)), 177-183, 2023, https://doi.org/10.1007/978-981-99-2742-5_19
[13] Narayan Patra, JitendraPramanik,Abhaya Kumar Samal &Subhendu Kumar Pani, "Machine Learning Application in Primitive Diabetes Prediction—A Case of Ensemble Learning", Cognitive Science and Technology ((CSAT)), 177-183, DOIhttps://doi.org/10.1007/978-981-99-2742-5_192022
[14] T. R. Vibha, C. Saravanan & T. L. Divya, "Melanoma Skin Cancer Detection and Classification Using Deep Learning and Image Processing", SN Computer Science, volume 6, no 5, DOI:10.1007/s42979-025-04009-x. 2025.
[15] Anamika Jain, Akansha Singh & AmanDoherey, "Prediction of Cardiovascular Disease using XGBoost with OPTUNA", SN Computer Science, volume 6, no 5, DOI:10.1007/s42979-025-03954-x2025.
[16] Essam H. Houssein, Doaa A. Abdelkareem, Gang Hu Mohamed Abdel Hameed, Ibrahim A. IbrahimMinaYounan, "An effective multiclass skin cancer classification approach based on deep convolutional neural network", Cluster Computing (2024) 27:12799–12819 https://doi.org/10.1007/s10586-024-04540-1
[17] Dikai Li, "Attention-enhanced architecturefor improved pneumonia detection in chestX-ray images", Li BMC Medical Imaging (2024) 24:6, https://doi.org/10.1186/s12880-023-01177-1
[18] BurcuOltu, SeldaGüney, SenihaEsenYukselandBernaDengiz, "Automated classification of chest X-rays: a deep learning approach with attention mechanisms", Oltu et al. BMC Medical Imaging (2025) 25:71, https://doi.org/10.1186/s12880-025-01604-5
[19] Fabrizio Albertetti, Alena Simalastar &Aïcha Rizzotti-Kaddouri, "Stress Detection with Deep Learning Approaches Using Physiological Signals", Lecture Notes of the Institute for Computer Sciences, Social Informatics and Telecommunications Engineering ((LNICST,volume 360)).2021. https://doi.org/10.1007/978-3-030-69963-5_7
[20] Zankhana Bhatt & AshwinDobariya, "Stress Level Classification Using Multimodal Deep Learning and Physiological Signal Analysis", Lecture Notes of the Institute for Computer Sciences, Social Informatics and Telecommunications Engineering ((LNICST,volume 360)) 2025.
[21] CheanKhim Toa, Mahmoud Elsayed &KokSwee Sim, "Deep residual learning with attention mechanism for breast cancer classification", Applied Soft Computing, volume 28, 9025-9035, (2023).
[22] K. Paramesha, ShrutiJalapur, ShaliniHanok, Kiran Puttegowda, G. Manjunatha & Bharath Kumara, "Machine Learning and Deep Learning Approaches for Guava Disease Detection" SN Computer Science, volume 6, article no 361, 2025.
[23] Puttegowda Kiran, V. Veeraprathap, U. Rajashekhar, MathapatiMahantesh, K. V. Sudheesh, Kumara Bharath &K. Prabhavathi. "Optimized Machine Learning Techniques for

Precise Breast Cancer Detection in Mammograms", SN Computer Science, 6(4):1-22, DOI:10.1007/s42979-025-03933-2. 2025.
[24] AbdulahiMahammedAdem, Ravi Kant & Gaurav Gupta, "High-Level Ensemble: An Approach for Breast Cancer Classification", SN Computer Science, 6(4):DOI:10.1007/s42979-025-03844-2. 2025.
[25]V. Helen Deva Priya & A. Vimala Juliet, "A Deep Learning-Based Multiple Lung Disease Prediction and Classification Using CT- Scan Images", SN Computer Science, volume 6, article 367, 2025, https://doi.org/10.1007/s42979-025-03915-4
[26] Chiranjeevi Karri, JoãoSantinha, Nikolaos Papanikolaou, Santosh Kumar Gottapu, Manohar Vuppula, P. M. K. Prasad, "Pancreatic cancer detection through semantic segmentation of CTimages: a short review", Discover Artificial Intelligence, (2024) 4:101, https://doi.org/10.1007/s44163-024-00148-x
[27] Francis AdobaEkle, Vincent Shidali, Richard EmocheOchogwu,Igoche Bernard Igoche, "Machine Learning models for heart disease prediction and dietarylifestyle change therapy recommendation: a systematic review", Discover Artificial Intelligence, (2024) 4:113 | https://doi.org/10.1007/s44163-024-00181-w
[28] Krishan Kumar, Kiran Jyoti, Krishan Kumar, "Machine learning for brain tumor classification: evaluating featureextraction and algorithm efficiency", Discover Artificial Intelligence (2024) 4:112 ,https://doi.org/10.1007/s44163-024-00214-4
[29] Md. RezaulIslam,Aniruddha Islam Chowdhury, SharminShama, Md. Masudul Hasan Lamyea, "Enhanced thyroid disease prediction using ensemble machinelearning: a high-accuracy approach with feature selection and classbalancing", Discover Artificial Intelligence (2025) 5:9 | https://doi.org/10.1007/s44163-025-00225-9.
[30] HajarRabie,Moulay A. Akhloufi, "A review of machine learning and deep learning for Parkinson'sdisease detection", Discover Artificial Intelligence (2025) 5:24https://doi.org/10.1007/s44163-025-00241-9.
[31] Sumita Lamba, Satender Kumar, Manoj Diwakar, "FADLEC: feature extraction and arrhythmia classification using deeplearning from electrocardiograph signals", Discover Artificial Intelligence (2025) 5:82 https://doi.org/10.1007/s44163-025-00290-0
[32] Zulfikar Ali Ansari, Manish MadhavaTripathi, Rafeeq Ahmed, "The role of explainable AI in enhancing breast cancer diagnosis usingmachine learning and deep learning models", Discover Artificial Intelligence (2025) 5:75 https://doi.org/10.1007/s44163-025-00307-8
[33] FarnazHoseini,AnaramYaghoobiNotash, "Image captioning using bidirectional LSTM neural network", Discover Artificial Intelligence (2025) 5:80 https://doi.org/10.1007/s44163-025-00315-8
[34] Emmanuel Ahishakiye, Fredrick Kanobe, "Breast cancer classification using breast ultrasound imageswith a hybrid of transfer learning and Bayesian-optimized fastlearning network", Discover Artificial Intelligence (2025) 5:81 https://doi.org/10.1007/s44163-025-00335-4
[35] RabiaJaved, Tahir Abbas, Ali Haider Khan, Ali Daud,Amal Bukhari, RiadAlharbey, "Deep learning for lungs cancer detection: a review", Artificial Intelligence Review (2024) 57:197https://doi.org/10.1007/s10462-024-10807-1
[36] Boon Feng Wee,SaaveethyaSivakumar, King Hann Lim, W. K. Wong, Filbert H. Juwono, "Diabetes detection based onmachine learning and deeplearning approaches", Multimedia Tools and Applications (2024) 83:24153–24185, https://doi.org/10.1007/s11042-023-16407-5
[37] Helena Liz-López,ÁureaAnguera de Sojo-Hernández, Sergio D'Antonio-Maceiras,

Miguel Angel Díaz-Martínez, David Camacho, "Deep Learning Innovations in the Detection of Lung Cancer: Advances,Trends, and Open Challenges", Cognitive Computation (2025) 17:67https://doi.org/10.1007/s12559-025-10408-2
[38] YogeshKumaran S, J. Jospin Jeya, Mahesh T R, Surbhi Bhatia Khan, Saeed Alzahraniand Mohammed Alojail, " Explainable lung cancer classification with ensemble transfer learning of VGG16, Resnet50 and InceptionV3 using grad-cam", BMC Medical Imaging (2024) 24:176 https://doi.org/10.1186/s12880-024-01345-x
[39] JayeshGangrade, RajitKuthiala, Shweta Gangrade, YadvendraPratap Singh, Manoj R&Surendra Solanki, "A deep ensemble learning approach for squamous cell classification in cervical cancer", Scientific Reports| (2025) 15:7266 https://doi.org/10.1038/s41598-025-91786-3
[40] NanaNyarkoBrenya Appiah Kubi,SajidNazir, "Dementia prediction with multimodal clinical and imaging data", International Journal of Information Technology (2025) 17:5–16 https://doi.org/10.1007/s41870-024-02326-7.
[41] Leelavathi Arepalli,Venkata Rao Kasukiurthi & Madhavi Dabbiru, "Channel boosted Convolution Neural Network with segment based Segmentation for an automatic prediction of Thyroid Cancer ", Soft Computing, Volume 29, 2399-2415, 2025.https://doi.org/10.1007/s00500-025-10482-6.
[42] Hossam Magdy Balaha, Asmaa El-Sayed Hassan, Rawan Ayman Ahmed & Magdy Hassan Balaha, "Comprehensive multimodal approach for Parkinson's disease Classification using Artificial Intelligence: Insights and model explainability", Soft Computing, Volume 29, 1845-1877, 2025, https://doi.org/10.1007/s00500-025-10463-9
[43] Pranab Sahoo, Sriparna Saha, Saksham Kumar Sharma & Samrat Mondal, "Boosting Carvical Cancer Detection with a multi-stage architecture complementary information fusion", Soft Computing, Volume 29, 2025, 1191-1206, https://doi.org/10.1007/s00500-025-10491-5.
[44] HarikaVanam, G. Vijaylaxmi & VanamSravan Kumar, "Automated cervical Cancer Classification using Stacked BI-LSTM and optimized spiking Neural Network with deer hunting Optimization Algorithm",InternationalJournal of Information Technology (2025), May 2025, https://doi.org/10.1007/s41870-025-02579-w
[45] IshakPacal & SerhatKılıcarslan, "Deep Learning based approaches for robust classification for cervical Cancer",International Journal of Information Technology, 2023, volume 23, 18813-18828, https://doi.org/10.1007/s00521-023-08757-w.
[46] Rajwinder Singh, Hardeep Kaur & Jyoteesh Malhotra, "Cervical Cancer Detection through Pap Smear images using hybrid deep Feature Extraction and Ensemble Machine Learning", International Journal of Information Technology, volume 8, article number 233, 2025. https://doi.org/10.1007/s41939-025-00834-y
[47] Hafsa Binte Mahbub, Akeem Olowolayemo, Swaleh Maulid Omari & Imran AdemolaAdeleke, "Invasive ductal carcinoma(IDC) Detection in Breast histopathology images using Enhanced Transfer Learning of Convolution Neural Network", International Journal of Information Technology, 2025, https://doi.org/10.1007/s41870-025-02522-z
[48] S. Shanthi, J. A. Smitha & S. Saradha, "Automatic Lung Cancer Detection and classification using Modified Golf Optimization with DenseNet Classifier", International Journal of Information Technology, 2024, volume 17, 1551-1559, https://doi.org/10.1007/s41870-024-01950-7
[49] Sunil Kumar K N, Pavan P. Kashyap, Darshan A. Bhyratae, Suhas A. Bhyratae & A. Kalaivani "CNN-BO-LSTM an ensemble Framework for prognosis of Lever Cancer", International Journal of Information Technology, 2024, volume 17, 1103-1109, https://doi.org/10.1007/s41870-024-02190-5
[50] Gedeon Kashala Kabe, Yuqing Song & Zhe Liu, " FireNet-MLstm for classifying lever lesions using Deep Features in CT Images", Multimedia Tools and Applications (2022) 81:1607–1623, https://doi.org/10.1007/s11042-021-11411-z

[51] Munipraveena Rela, Nagaraja Rao Suryakari &Ramana Reddy Patil, "A Diagnosis System by Unet and Deep Neural Network enabled with optimal feature selection for lever tumour detection using CT images"Multimedia Tools and Applications (2023), Volume 82, pages 3185-3227, https://doi.org/10.1007/s11042-022-13381-2
[52] Mingfang Hu, Shuxin Wang, Mingjie Wu, Ting Zhuang, Xiaoqing Liu & Yuqin Zhang, "Automatic Classification of Focal Lever Leisons based on Multi Sequence MRI", Journal of Imaging Informatics in Medicine, 2024, https://doi.org/10.1007/s10278-024-01326-0
[53] Abolfazl Bagheri Tofighi, Abbas Ahmadi & Hadi Mosadegh, "Improving Lung Cancer Detection via MobileNet V2 and Stacked-GRU with explainable AI", International Journal of Information Technology, 2024, 1189-1196, https://doi.org/10.1007/s41870-024-02045-z.
[54] Madhab Paul Choudhury, J. Paul Choudhury, *"*A Framework for Developing Correct Software Programs through Software Defect Prediction and Elimination using Machine Learning Models*"*, International Journal for Research in Applied Science Engineering Technology (IJRASET), ISSN: 2321-9653; IC Value: 45.98; SJ Impact Factor: 7.538, Volume 12 Issue IX Sep 2024, page 402-411
[55] Madhab Paul Choudhury, J. Paul Choudhury, "A Comparative performance of Machine Learning models with cross validation techniques for the prediction lever disease",
Journal Of Technology, Issn No:1012-3407 || Vol 15 Issue 5, impact factor 4.6, pages 1-37
[56] Retinal Fundus Image Data Set:
https://www.kaggle.com/datasets/kssanjaynithish03/retinal-fundus-images